Exoplanet Detection

Learners' Space Astronomy

Contents

1 Introduction **3**
- 1.1 What Are Exoplanets? . . . 3
- 1.2 Why do we Care? . . . 3

2 Early Discoveries **5**
- 2.1 The First Confirmed Exoplanet . . . 5
- 2.2 A Miraculous Discovery . . . 7
- 2.3 Detection Techniques . . . 8

3 Pulsar Timing **9**
- 3.1 Introduction . . . 9
- 3.2 Theory . . . 9
- 3.3 Discoveries . . . 13

4 Direct Imaging **14**
- 4.1 Introduction . . . 14
- 4.2 Problems . . . 16
- 4.3 Targets and Inferences . . . 18
- 4.4 Techniques . . . 19
  - 4.4.1 Aperture, SNR and Resolution . . . 19
  - 4.4.2 Coronagraphs and Adaptive Optics . . . 21
  - 4.4.3 Infrared imaging . . . 22
- 4.5 Discoveries . . . 25

5 Gravitational Microlensing **26**
- 5.1 Introduction . . . 26
- 5.2 Theory . . . 28
  - 5.2.1 Microlensing: Context . . . 28
  - 5.2.2 Basics of Lensing . . . 29
  - 5.2.3 Exoplanets from microlensing . . . 31
- 5.3 Discoveries . . . 35

6 Astrometry **36**
- 6.1 Introduction . . . 36
- 6.2 Theory . . . 36
  - 6.2.1 Measurement Principles and Accuracies . . . 36
  - 6.2.2 Inferences . . . 38

6.3 Discoveries 45

7 Transits **46**
7.1 Introduction 46
7.2 Theory 47
7.2.1 Transit Probability 48
7.2.2 Measurements, Error and Limits 49
7.2.3 Limb Darkening 51
7.2.4 Transit Light Curves 53
7.3 Discoveries 54

8 Radial Velocity **56**
8.1 Introduction 56
8.2 Theory 57
8.2.1 Orbits 57
8.2.2 Measurements, Error and Limits 59
8.2.3 Radial Velocity Curves and Information Obtained 64
8.3 Discoveries 65

9 Advancement in Technology **67**
9.1 The Future of Exoplanet Detection 67
9.1.1 Advancements in Exoplanet Detection Technology 67
9.2 Exoplanet Detection Using Machine Learning 67
9.2.1 Deep Dive 68

10 Conclusion and Extra Reading **69**

Introduction

1.1 What Are Exoplanets?

Exoplanets or Extrasolar Planets, as the name suggests, are planets, beyond our solar system.

What does that really mean though? To get a clear idea, we need to know what a planet actually is. According to the IAU (International Astronomical Union), to be called a Planet a celestial entity:

- Must be in orbit around a star
- Has sufficient mass for its self-gravity to overcome rigid body forces so that it assumes a hydrostatic equilibrium (nearly round) shape
- Has cleared the neighbourhood around its orbit (The entity is massive enough to throw any other comparable-size objects out of its orbit, such that its orbit is "cleaned up" of said objects)

This is the currently accepted definition, and is subject to change as debate and discoveries continue.

1.2 Why do we Care?

Other than the mind-numbing notion that we're standing on but one of trillions of such roughly spherical wanderers hidden in plain sight, Everything we think we know about the origins of Planets, each with their own composition, atmosphere, cycles, and systems is constantly being challenged as we discover these new worlds.

We know the Earth has limited resources. Largely science fiction at this point, but if we were to leave an uninhabitable earth in the future, if we could, where would we go?

Are we alone in the Universe? A question so famous, yet unanswered! We're the first generation who has the tools at our fingertips to begin to answer this question with scientific observations, and turns out we're lucky enough to witness the first steps of this cosmic-scale search.

To answer these big questions, we must know where to start, and that's what we're going to discuss here. We'll look at the beginning of the exoplanet hunt, the methods of detection developed over time, as well as the mathematics involved with them.

A few links to get you interested in this module (In case our words weren't enough ;-;)

- https://www.youtube.com/watch?v=EUU0-ZpFoK4
- https://exoplanets.nasa.gov/alien-worlds/strange-new-worlds/
- https://exoplanets.nasa.gov/alien-worlds/exoplanet-travel-bureau/

The primary goal of this study is to detect Exoplanets. Ideally, we'd want to know as much about these faraway masses as we do about our own planet. Sadly that isn't possible, but we'll probably get there. Here are a few essential aspects of exoplanets studied.

- **Detection and Confirmation**: The primary goal is to detect and confirm the existence of exoplanets.
- **Orbital Parameters**: Determining the orbital parameters of an exoplanet is crucial for understanding its dynamics and environment. In a discussion on orbits up ahead, our goal is to determine properties such as eccentricity, inclination, semi-major axis, and more, parts of which can be determined by every method.
- **Size and Mass**: Measuring the size and mass of exoplanets provides insights into their density, composition, and structure. Transit photometry and radial velocity methods can be used to estimate the size and mass of exoplanets, allowing scientists to classify them as rocky, gaseous, or potentially even icy.
- **Atmosphere**: Studying the atmosphere of exoplanets is essential to assess their habitability and potential for supporting life. Observations through spectroscopy can reveal the chemical composition, presence of certain gases, and even potential signs of biological activity in the atmosphere. This can be done through techniques such as transmission spectroscopy and emission spectroscopy.
- **Habitability and Extraterrestrial Life**: Scientists are interested in identifying exoplanets within the habitable zone of their host star, where conditions might allow the presence of liquid water—an essential ingredient for life as we know it. Factors like the exoplanet's distance from its star, stellar radiation, and atmospheric properties are studied to assess its potential habitability. However, habitability and presence of lifeforms is a complex domain of study. Extraterrestrial life is a field of the future, If we last long enough to see it through :).

Early Discoveries

For centuries scientists, philosophers, and science fiction writers suspected that extrasolar planets existed, but there was no way of knowing whether they were real in fact, how common they were, or how similar they might be to the planets of the Solar System. Various detection claims made in the nineteenth century were rejected by astronomers.

A few discredited claims before the first exoplanet confirmation (if you want to know):

- https://en.wikipedia.org/wiki/70_Ophiuchi
- https://en.wikipedia.org/wiki/Barnard%27s_Star
- https://en.wikipedia.org/wiki/PSR_B1829%E2%88%9210

Claims were usually refuted, as they heavily relied on Astrometric techniques (we'll learn more about this later), which given the accuracy of the time, were much less reliable than they are today.

2.1 The First Confirmed Exoplanet

The first exoplanet to be confirmed was a rather uncommon case, considering the methods we have today, which target mostly the main sequence stars in the middle of the HR diagram. This one was found orbiting a Pulsar.

Pulsars are thought to be highly magnetised neutron stars left behind after supernovae, the death of stars many times more massive than our sun. Because they constitute most of the star's mass (they are the compressed core of the star after all), in a radius of a few kilometres, the conservation of angular momentum explains the high speeds at which these rotate, skew to their magnetic axis. These pulsars release high-power beams of accelerated charged particles (EM Radiation) from their magnetic poles. This results in a periodic signal of electromagnetic pulses which we can observe from Earth at a safe distance. These have a period of a few milliseconds to a few seconds, which are more precise and regular than atomic clocks!

In the late 1980s, Aleksander Wolszczan and Dale Frail observed the Pulsar PSR B1257+12, noticing minute fluctuations in its time period. Previous discoveries (Hulse-Taylor Binary Pulsar) alluded to the presence of a surrounding body, which caused the Pulsar to "wobble" about the common centre of mass causing these small changes (We'll look at this method in more detail later).

A few years later in 1992, PSR B1257+12 c, Poltergeist and PSR B1257+12 d, Phobetor became the very first exoplanets to be confirmed. You can learn about the nomenclature of exoplanets here.

With only 50 out of today's discovered 5000+ Exoplanets detected using Pulsar Timings, you can see how rare these things are. Only special processes can give rise to planet-sized companions around pulsars, and many are thought to be exotic bodies such as planets made of diamond that were formed through the partial destruction of a companion star!

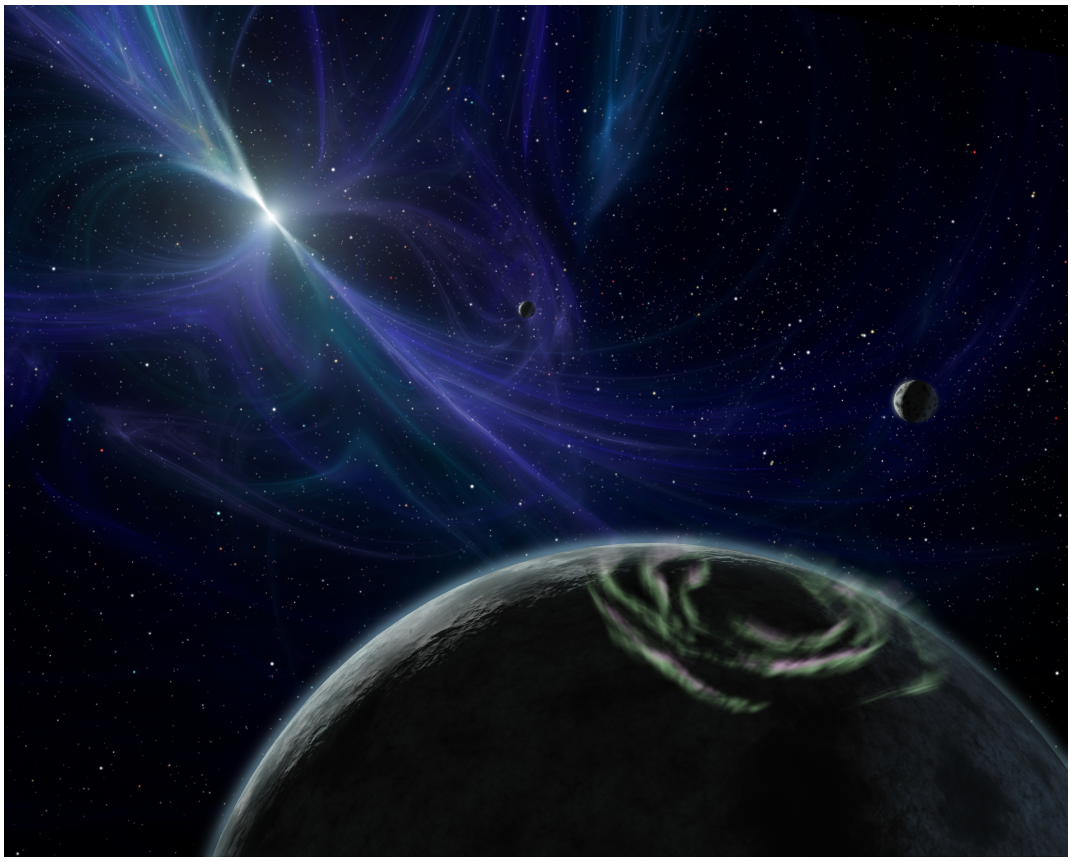

Figure 2.1: Artist impression of PSR B1257+12 system.

Even before this, back in 1989, astronomers who were monitoring a set of stars in order to create a list of good radial velocity standards noticed that one of their objects showed small, periodic changes in its velocity. The authors realized that the perturbing object might have a mass small enough to prevent it from fusing hydrogen, and so it might be a planet - HD 114762 b... but they noted that without a measured inclination for the orbit, it might very well NOT be a planet. Continued monitoring of the host star has failed to detect transits of HD 114762 by this orbiting body, and so we still don't know the inclination. Since the lower bound on the object's mass does (barely) fall within the planetary range, some lists and databases do call it a "planet."

2.2 A Miraculous Discovery

3 years later, in 1995, while searching bright stars for evidence of exoplanets, Didier Queloz and Michel Mayor came across 51 Pegasi. They were using the radial velocity method (which we'll discuss later), now the most popular methods of exoplanet detection, but relatively new at the time.

51 Pegasi is a G5-V type star, or a class G main sequence star (remember the HR diagram), which is very similar to our sun, a G2-V type star. With only our Solar system to go off of, and no exoplanets ever reported around sun-like stars, Didier and Michel had a hard time believing their measurements!

51 Pegasi b, the gas giant which earned these two the Nobel prize for various reasons, which looked nothing like anything in our Solar System, was a "Hot Jupiter", a type of planet that had been thought to exist but never confirmed. What made it significant was its mass (approximately half that of Jupiter), proximity to its host star, 51 Pegasi, and its short orbital period of about 4.2 days! It was also the first-ever exoplanet to be confirmed orbiting a Sun-like star.
A few links for your interest:

- Significance of 51 Peg b
- HR Diagram
- Types of Exoplanets
- NASA eyes on exoplanets
- NASA Exoplanet Archive

Since then, around 5400 exoplanets have been discovered, most of them around main sequence stars of spectral categories F, G and K i.e. in the middle of the HR diagram. This is because:

- They are abundant, more stable and live longer
- In expensive planet search missions, to identify as many exoplanets as possible, it's clear we should target the ones with the easiest measurements.
- Statistical analyses indicate that lower-mass stars (red dwarfs, of spectral category M) are less likely to have planets massive enough to be detected by the radial-velocity method, which is used often. Transit probabilities are also low.
- Hotter O, B and A types are much more massive than their orbiting bodies. As a result, the effect of their exoplanets on observables is less pronounced. However, with technological advancements, these planets are also being probed.

But a majority of these exoplanetary systems are very different from our Solar System!

- The orbits of all the major planets of our Solar System are quite close to being circular (apart from Pluto's, which is a special case).
- The four giant planets are a considerable distance from the Sun. The extrasolar planets detected so far - all giants similar in nature to Jupiter – are by comparison much closer to their parent stars, and their orbits are almost all highly elliptical and so very elongated.
- No other discovered planetary system has as more planets than our own, this directly correlates with the first point, which is highlighted nicely here

2.3 Detection Techniques

There are 7 basic methods used to detect exoplanets, each suited to different kinds of stars and having their limitations and advantages, out of which we'll be discussing the first 6, which are the most popular, and in use.

These are:

- Pulsar Timing
- Direct Imaging
- Gravitational Microlensing
- Astrometry
- Transits
- Doppler Method / Radial Velocity method
- Orbital Brightness variation

Keep in mind that multiple methods may be utilised to confirm the existence of an exoplanet. Radial velocity is frequently used to confirm potential candidates.

These methods are often complemented by follow-up observations and additional characterization techniques, such as spectroscopy, to determine the properties of exoplanets, including their masses, atmospheres, and compositions.

Pulsar Timing

3.1 Introduction

An orbiting planet causes the periodic oscillation of the position of the host star about the system's barycentre, recognisable through changes in the radial velocity and astrometric position of the primary. This forms the basis for the corresponding methods of detection.

However, If the host star also possesses some kind of periodic time signature(s), then these can provide an alternative method to detect orbiting planets through the change in measured period due to light travel time.

There are three classes of objects which offer this possibility:

- Radio Pulsars
- Pulsating Stars - These are stars, the brightness of which varies periodically due to internal or external factors (mostly internal as in Cepheid Variables and RR Lyrae Variables).
- Eclipsing Binaries - Binary star systems which have an orbital plane somewhat aligned with the Line-of-sight of Earth.

In this module, we shall only be looking at Pulsars as an example, particularly millisecond pulsars. Millisecond pulsars, which can be timed with high precision, have a stability comparable to atomic-clock-based time standards when averaged over decades.

True to their name, they have very short time periods, of the order of milliseconds. They aren't normal pulsars, which rotate noticeably slower. These are 'recycled' old ($\sim 10^{-19}$ yr old) neutron stars that have been spun-up to very short periods during mass and angular momentum transfer from a binary companion and have large slowdown times.

3.2 Theory

When we measure pulses, at a particular frequency, we'll get a series of peaks along with noise. From this information, we can derive timing residual graphs (How). Timing residuals are the

difference between measured arrival time of the pulse and expected arrival time.

Considering 1 planet only, the change in measured period of oscillation of the Primary (Host pulsar) due to light travel time (The delay caused by the light coming to us having to travel different distances for different pulses), has an amplitude related to displacement of the Primary along the Line-of-Sight from Earth, given by (Perryman, 2011, p.75):

$$\tau_p = \frac{1}{c}\frac{a \sin i \, M_p}{(M_\star + M_p)} \approx \frac{1}{c}\frac{a \sin i \, M_p}{M_\star} \tag{3.1}$$

Where a is the semi-major axis of the Planet's orbit, M_p is the mass of the planet, $M_\star$ is the Stellar mass, i is the angle of inclination of the orbit and c is the speed of light.

Here τ_p is also known as arrival timing residual amplitude, and it is the maximum deviation of the observed time of arrival of the pulse of the pulsar from the predicted time of arrival (which is Time of previous pulse + Time period).

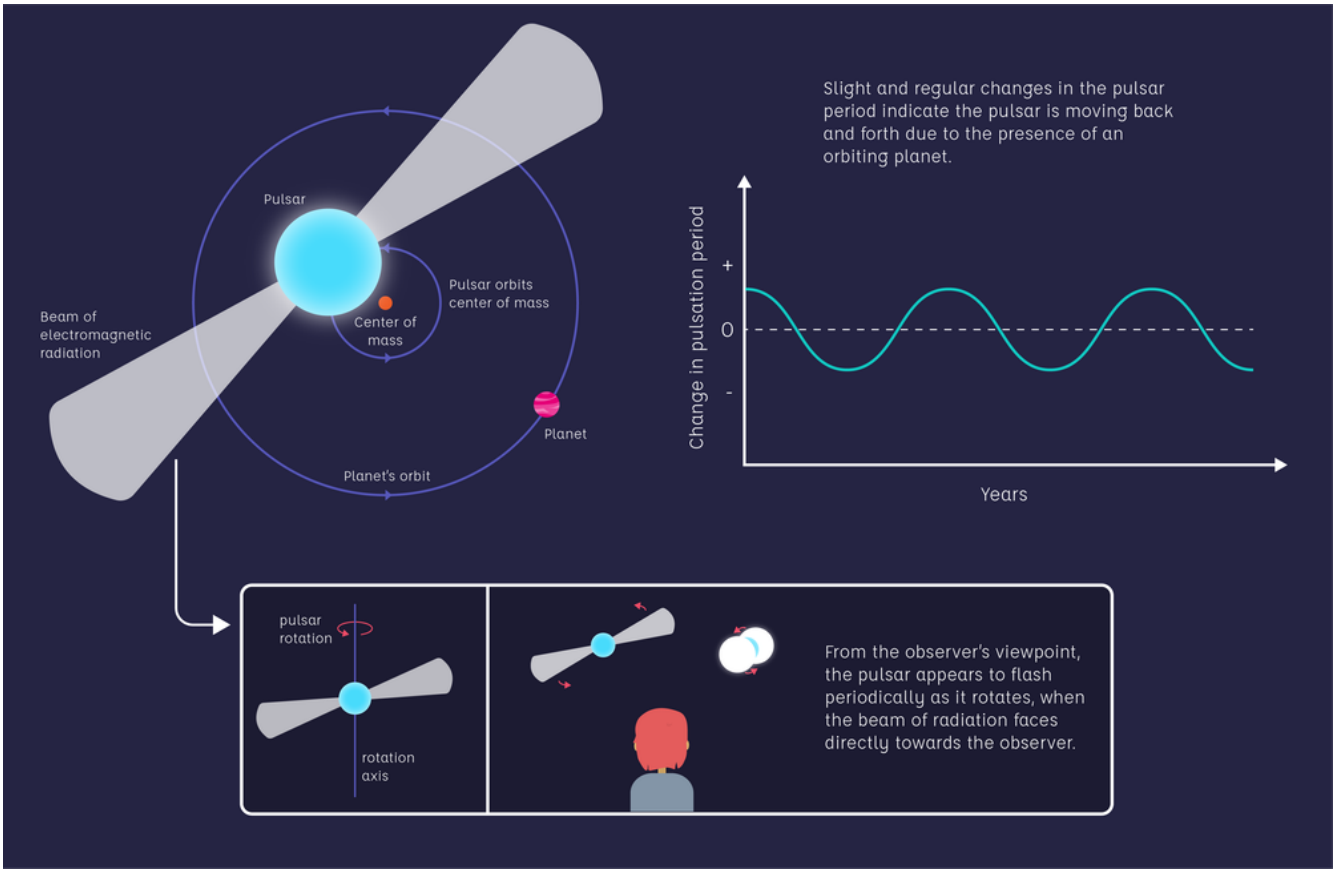

Figure 3.1: Pulsar Timing method

The stellar mass can be approximated from its Luminosity and other qualities, which leaves i and M_p as the only variables. Unfortunately this is where we hit a dead end. The effect of the movement will only be seen if there is motion along the Line of Sight of earth, hence in a face on orbit, there's nothing we would see. Due to this limitation we can only hence put a lower limit

on $M_{p(obs)} = M_{p(real)} \sin i$. $M_{p(real)}$ and i cannot be determined separately by this method, and we must resort to other ways to determine i.

This is obviously ideal, and for a single planet, which is rarely the case. Let's talk about actual measurements.

Pointing our radio telescopes to a particular pulsar, we see peaks and noise. Given the accuracy of pulsars, you may expect the timing residual graph to be a flat line if there are no planets, but...we get something like this:

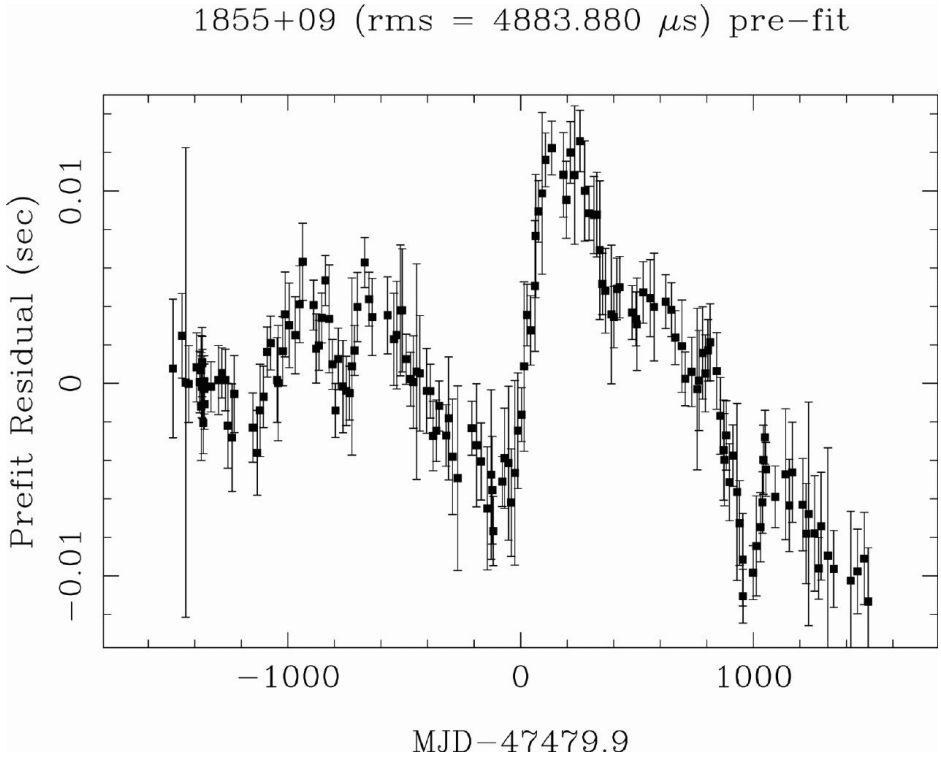

Figure 3.2: Observed 'Pre-fit' timing residuals for a random pulsar (values on x-axis indicative of years), Credit

Various reasons for fluctuations seen in pulsar residuals are a constant spin-down of pulsars, the earth's motion, proper motion of the pulsar, Parallax, sudden random increases in rotation speed followed by a period of relaxation, called 'glitches'; and low frequency stochastic deviations on a time scale of hours to years called 'Timing Noise'. Even exoplanet satellites may introduce higher order changes in the residuals!
These fluctuations have to be removed by developing models to 'fit out' the residuals caused by them. Basically, as you account for more and more of these factors and remove them from your readings, the residual graph tends more and more towards a straight line.

(How might these factors influence our graph? The document linked to here lists the various delays (fluctuations in timing residuals) that may be involved with pulsar timing measurements.)

However, in rare cases, you might be left with this:

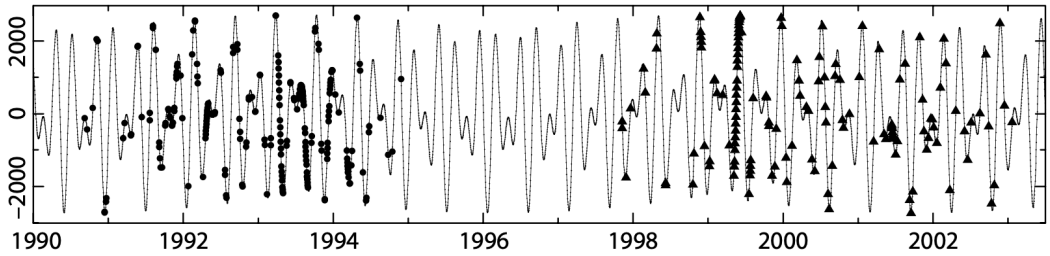

Figure 3.3: Daily-averaged arrival time residuals for PSR B1257+12 observed at 430 MHz with the 305-m Arecibo radio telescope between 1990–2003: residuals for a model without planets. Y-axis values in μs(residuals), X-axis values indicate year (Perryman, 2011, p.76).

This is how you know your pulsar isn't alone. This graph is for the residuals left after fitting out the residuals of a Pulsar model without planets. Keplerian planetary models, with different number of planets, masses and orbital parameters are developed to, again, fit out the residuals until you're left with a flat line. the best fitting parameters can give you information about the planets.

Since we have been talking about PSR B1257+12, let's take this as an example case:

The first planet discovered around an object other than the Sun was found around the 6.2-ms pulsar PSR B1257+12 at d∼300 pc, At least two terrestrial-mass companions were inferred, with masses of $M \sin i \approx 2.8$ and $3.4 M_{\oplus}$. Their orbits were almost circular, with $a = 0.47$ and 0.36 AU.

How could they absolutely be sure of their planet hypothesis? Although a number of alternatives to explain the observed timing residuals were examined, the planet hypothesis could be rigorously verified: the semi-major axes of the orbits are sufficiently similar that the two planets would perturb one another significantly during their orbital close encounters, every ∼200d, with resulting three-body effects leading to departures from a simple non-interacting Keplerian model which would grow with time. The model was confirmed by continued monitoring.

Modeling of the orbit evolution also allowed masses to be derived without a priori knowledge of their orbital inclination, i :)

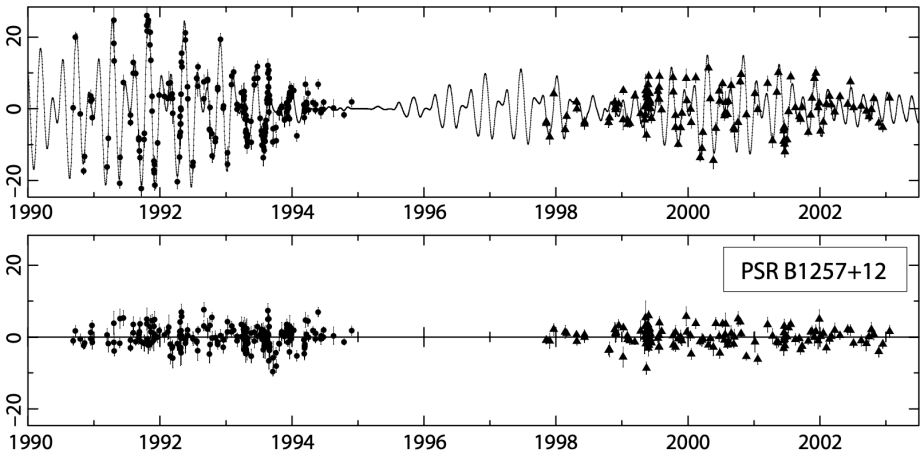

Figure 3.4: Timing Residuals for PSR B1257+12. Top: Residuals for a Keplerian model for all three planets, dominated by perturbations between the outer planets. Bottom: residuals after inclusion of planet–planet perturbations (Perryman, 2011, p.76)

You can see that even after fitting a model to the data obtained, the final residuals look like a random scatter of values around an average of 0, with no discernible patterns.

3.3 Discoveries

As mentioned before, the PSR B1257+12 system was truly a significant discovery, but it isn't the only one. Around 50 extrasolar planets have been confirmed through pulsar timings. Most of these are massive, and orbit close to their parent neutron star, compared to planets around main sequence stars. The environments of these planets are likely extreme, subject to intense radiation and gravitational forces due to the fast spinning pulsar's strong field. The way of formation of these planets remains a topic of research and debate.

Direct Imaging

4.1 Introduction

Imaging generally refers to the detection of a point source image of the exoplanet. This may be either in the reflected light from the parent star (in the visible), or through its own thermal emission (in the infrared). This is to be distinguished from spatial resolution of an exoplanet surface, i.e. when we talk about imaging an exoplanet, the angular span of the planet itself on the earth isn't of importance to us (which is needed while obtaining spatial resolution of a planet surface), our job is solely to detect it as a point in the sky.

The scientific interest of obtaining exoplanet images is to confirm the accumulating but generally indirect evidence for their existence, which encourages more extensive spectroscopic investigations, and as a first step towards a future goal of obtaining resolved spatial imaging of an exoplanet surface.

If we want to directly image an exoplanet, we want to find something like this:

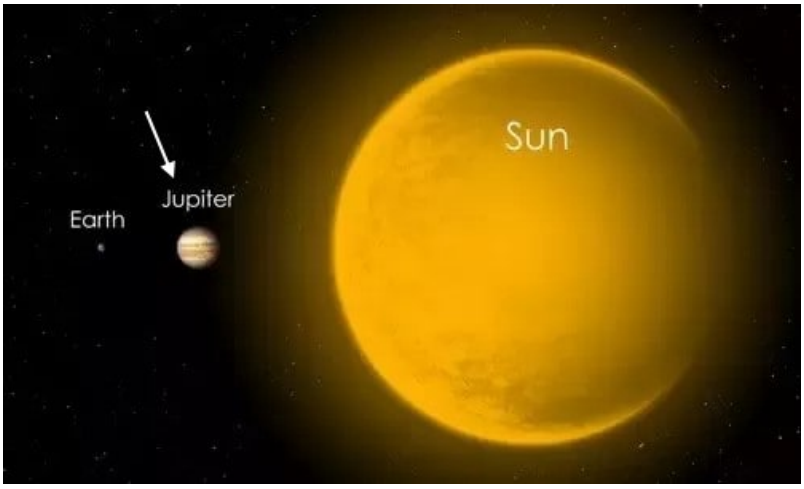

Figure 4.1: A Size Comparison

In this:

Figure 4.2

With a resolution like this:

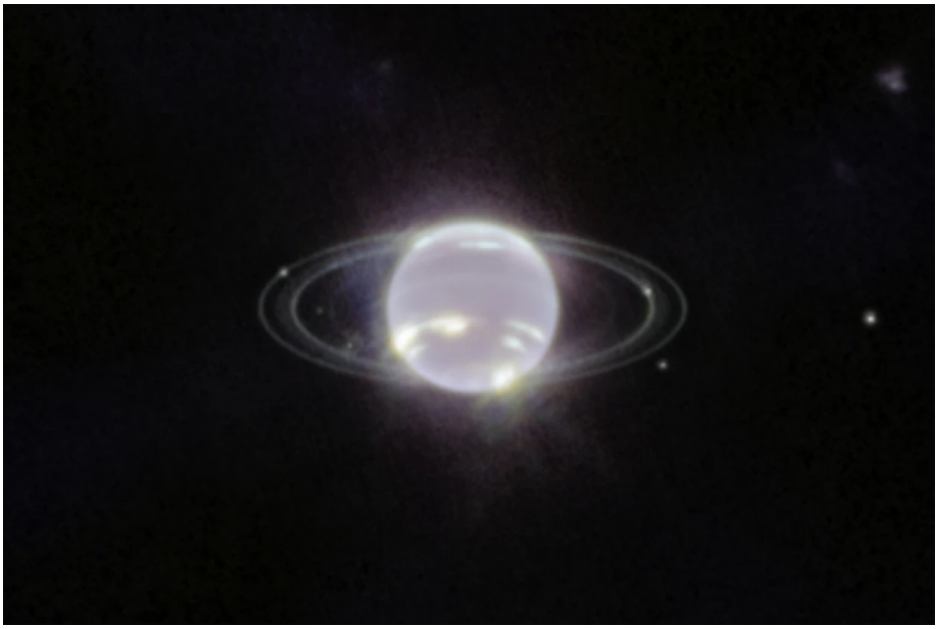

Figure 4.3: JWST image of Neptune's rings, Credit

But again, our purpose is to detect, not image the surface, If we're able to spot the reflected visible radiation or thermal emission of a body close to a star, then that suffices.

What all do we need to consider while taking such images, and what problems might we face? What we need to do is clear, why we it is difficult, and how to get better is important here.

4.2 Problems

What we see from earth is the apparent magnitude of celestial entities, and in this context it becomes imperative to talk about the relative brightness of the planet and star .The ratio of the planet to stellar brightness depends on the stellar spectral type and luminosity class, the planet's proximity to the star given by its orbital semi-major axis (a) and instantaneous projected separation, on the planet's mass, composition, radius (R_p) and age, on the scattering properties of its atmosphere, and on the observation wavelength. For reflected light of wavelength , the planet/star flux ratio can be written:

$$\frac{f_p(\alpha,\lambda)}{f_\star(\lambda)} = p(\lambda)\left(\frac{R_p}{a}\right)^2 g(\alpha) \tag{4.1}$$

(flux, or brightness is the Luminosity (power) of the source divided by the Area in which it is spread out, remember JEE questions involving radiation!).

where g(α) is a phase-dependent function, where α is the phase angle, and p(λ) is the geometric albedo of the planet (wavelength-dependant).

The specific form of the phase function depends on the scattering and reflective properties of the planet's atmosphere or surface. It describes how the reflected light from the planet varies with different phase angles. This received light is characterised by a phase curve, which is unique for each planet. Phase curves can be obtained for exoplanets through photometric and spectroscopic measurements, and modelling planets to fit to the curve. If the planet's thermal emission is significant, the emission phase function must be added as well.

In astronomy, the geometric albedo of a celestial body is the ratio of its actual brightness as seen from the light source (i.e. at zero phase angle) to that of an idealized flat, fully reflecting, diffusively scattering (Lambertian) disk with the same cross-section (Credits: Wikipedia). A Lambertian disk exhibits perfect diffuse reflection, i.e. no matter the direction you observe it from, the brightness observed will be the same. There is a particular function that represents this reflectance, this is Lambert's cosine law. Clearly, the albedo varies from 0 to 1. For a Lambert sphere (A sphere for which the overall brightness appears the same when viewed from every direction), the albedo is 2/3.

Our purpose in using this formula is just to get a rough estimate of contrast present in a star system, and infer the feasibility of probing the said star for exoplanets.

The star-planet angular separation depends on the orbital parameters as well as on the stellar distance. Exoplanets of interest (for various reasons), typically lie very close in angular terms to the host star, within 0.1 – 0.5 arcsec (the current best instruments like JWST can resolve objects with a separation of down to 0.1 arcsec), and are swamped by the bright stellar 'glare', the light from the star dominates the pixels which receive light from the system on the photodetectors used in telescopes. Planets further out from the host are consequently cooler, emit less and reflect less, even if they avoid the stellar glare, they are too dim to detect.

As an example, For the Jupiter–Sun system, the flux ratio is $\sim 10^{-9}$ at maximum elongation, in the mid-visible spectrum with an angular separation of 0.5 arcsec at 10 pc. Values for exoplanets of primary interest are expected to range from 10^{-5} in the infrared to 10^{-10} in the optical.

So, imaging the radiation from an exoplanet in the glare of a star is like trying to take an image of a firefly beside a lighthouse. A very bright idea (sorry). Hence, there are many problems associated with Direct imaging:

- The ratio $f_p/f_\star$ is very small.
- The temperature-varying atmosphere refracts the near parallel wavefront of light coming from the star irregularly, creating phase fluctuations and a distorted wavefront.
- Diffracted light from the telescope and supporting structures, and scattered light from wavefront aberrations which results in a residual intensity in the focal plane in the form of instrumental 'speckles'.

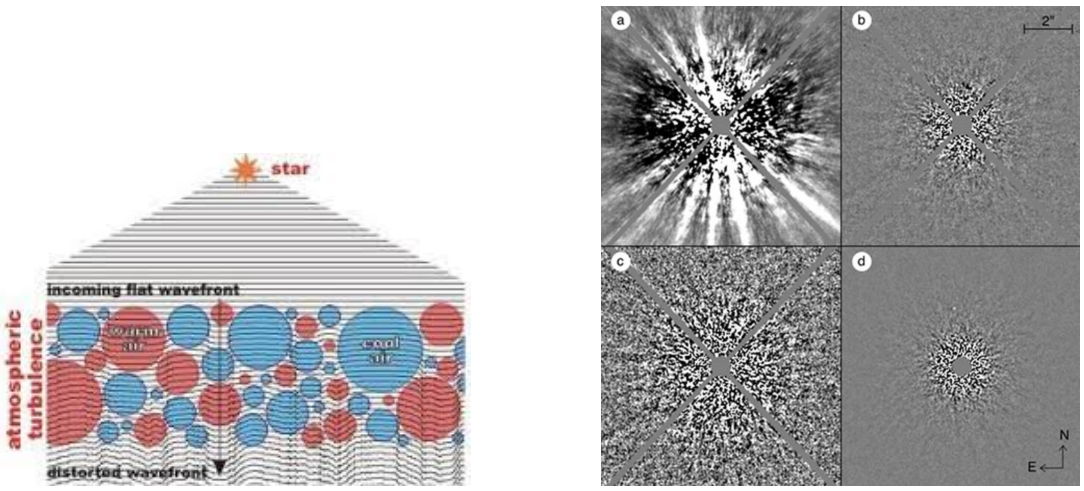

(a) Atmospheric wavefront distortions

(b) Speckle noise

Figure 4.4: Problems

Under these conditions elementary signal-to-noise calculations imply that obtaining a direct image of a planet is not feasible, and some means of removing or attenuating the starlight is required in order to improve the signal-to-noise ratio at the position of the planet.

4.3 Targets and Inferences

To date, the first images of massive, widely separated exoplanets have been acquired, although none so far resemble those of the solar system. The detection of exo-Earths remains out of reach of any of the imaging facilities currently under development. Facilities, like ground-based extremely large telescopes, JWST, and extreme 'adaptive optics' imagers, will instead focus on exoplanet categories where imaging prospects are highest, for example:

- Young stars (age 10–100Myr, distance d $<$ 100pc), around which the planets are still young, warm, and hence self-luminous.
- Stars with known planets, for which other methods suggest the existence of high-mass giant planets in wide-separation orbits.
- Nearby stars, d $<$ 5 pc, in which a shorter-period giant planet with significant reflected light might be detected because of its relatively large angular separation from the star due to its proximity.

Imaging planets and spectroscopy helps us obtain valuable information about the planet's mass, orbital parameters, temperature, atmosphere, phase curve and albedo.

The planets detected through direct imaging currently fall into two categories. First, planets are found around stars more massive than the Sun which are young enough to have protoplanetary

disks. The second category consists of possible sub-brown dwarfs found around very dim stars, or brown dwarfs which are at least 100 AU away from their parent stars.

Sometimes observations at multiple wavelengths are needed to rule out the planet being a brown dwarf. Direct imaging can be used to accurately measure the planet's orbit around the star. Unlike the majority of other methods, direct imaging works better with planets with face-on orbits rather than edge-on orbits, as a planet in a face-on orbit is observable during the entirety of the planet's orbit, while planets with edge-on orbits are most easily observable during their period of largest apparent separation from the parent star.

4.4 Techniques

Various techniques are being applied in attempts to image exoplanets at the highest angular resolution and contrast:

- Use of large apertures to improve signal-to-noise and resolution
- Coronagraphic masks to suppress light from the host star
- Adaptive optics to minimise the effects of atmospheric turbulence, or imaging from space to eliminate its effects altogether
- Interferometers to improve angular resolution, with "nulling interferometry" to eliminate the stellar light
- Improving contrast between the planet and star by observing at longer wavelengths.
- Post-processing to treat residual aberrations

We can't go into details of all of these, but we'll briefly discuss a few:

4.4.1 Aperture, SNR and Resolution

Noise associated with astroimaging includes shot noise, diffraction and aberrations by optical instruments, background radiation noise, and noise associated with the photodetector, such as dark current. This noise remains more or less constant with the change in the aperture for small apertures, while an increase in the aperture also increases the number of photons from the source the telescope is pointed towards, thus the Signal to noise ratio (SNR) increases, however for extremely large apertures the SNR decreases due to saturation of the pixels.

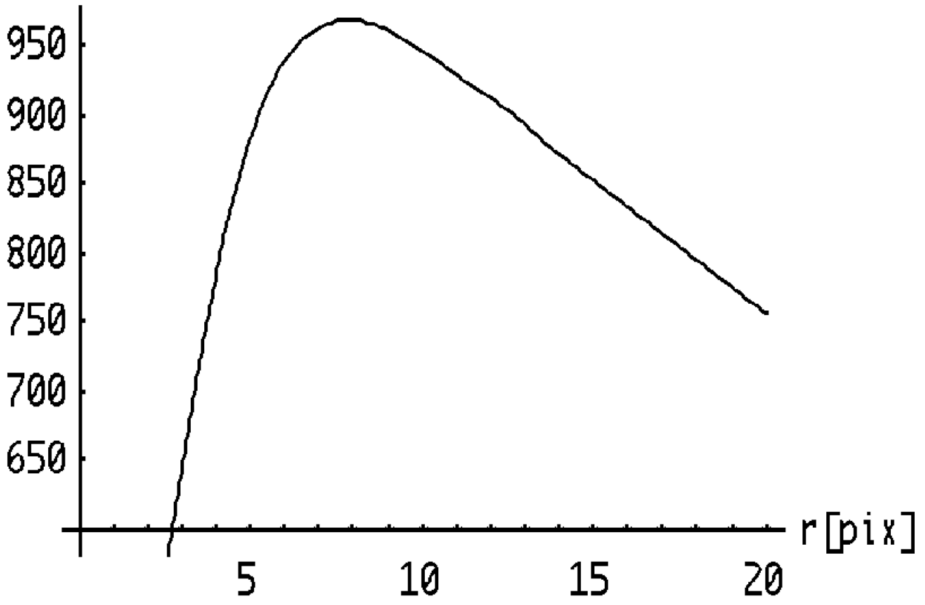

Figure 4.5: SNR (Y-axis) vs Radius of aperture, in terms of pixels for aperture photometry, Credit

---

The resolving power of an optical instrument determines its ability to distinguish separate images of closely spaced objects. Binary stars that appear as one to the naked eye can be clearly resolved into two distinct stars when viewed through a telescope.

When observing far-away objects, their images form diffraction patterns on the retina. If two objects are close together at a small angle , their diffraction patterns will overlap. Resolving the objects requires ensuring that the central maximum of one pattern falls onto the first minimum of the other pattern, known as the Rayleigh criterion. If the central maxima overlap, the objects will appear as one.

Figure 4.6

The width of the central maximum in a diffraction pattern depends on the aperture size, such as the pupil of the eye. Telescopes, with larger apertures, have greater resolving power. The minimum angular separation of two objects that can be resolved is given by $\theta_{min} = 1.22\lambda/D$, where

D is the diameter of the aperture. A good explanation of resolving power is given here.

Most observatories use reflector telescopes, originally designed to retain their shape solely by their thickness and intrinsic stiffness, a condition which limited maximum primary mirror diameters to 5m or so. Modern telescopes however make use of active optics, which involves monitoring the image over some time and chaging the shape of thinner mirrors or segmented mirrors using tiny pistons, to maintain an optimal shape.

4.4.2 Coronagraphs and Adaptive Optics

If the stellar glare is our problem, then we must find a way to block it. Here, we find inspiration in a natural phenomenon:

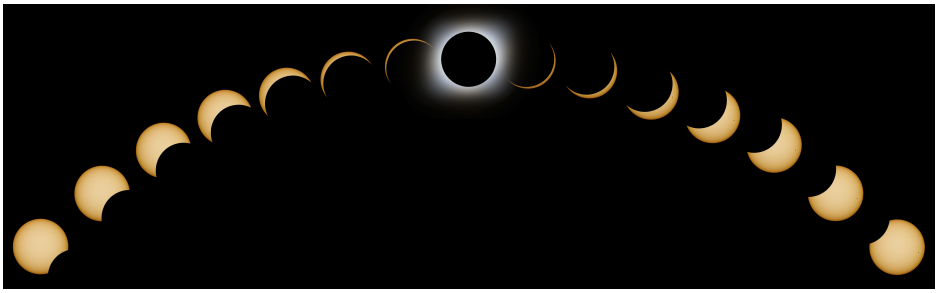

Figure 4.7: A Solar Eclipse

As the moon occults the disc of the Sun, the sun's glare is removed and we are able to see the fainter Corona. A Coronagraphic mask draws inspiration from this.

Obviously, a circular piece of cardboard in front of a telescope isn't enough for exoplanet imaging. The earliest design, which saw results in July 1991 was that of Bernard Lyot, the Lyot Coronagraph.

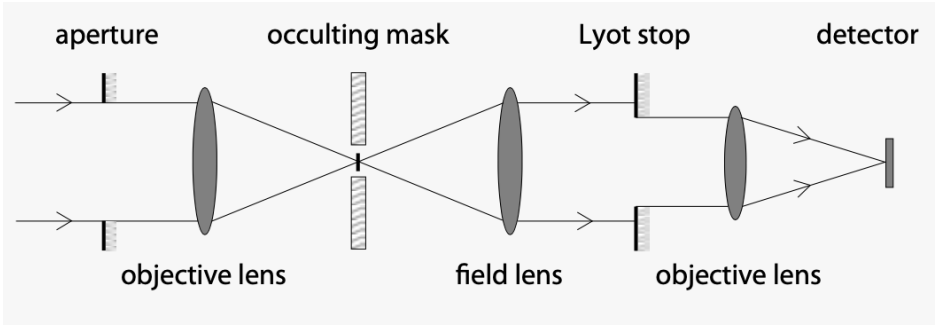

Figure 4.8: Schematic of the Lyot Coronagraph (Perryman, 2011, p.152)

The working of the Lyot Coronagraph is as follows: In the Lyot coronagraph as implemented for observations of the solar corona, the first objective lens forms an image of the disk and corona, and an occulting mask blocks the image of the disk.

If the occulting mask were the only blocking element, diffracted light at the edge of images would still cover faint off-axis structures. Consequently, a field lens re-images the objective lens and its diffraction pattern, and the 'Lyot stop' intercepts the diffraction ring while allowing most of the light from the surrounding structure to pass. The second objective lens relays the resulting image onto the detector plane. In a perfect Lyot coronagraph some 50% of the light from a nearby source might be lost, compared to the suppression of some 99% of the stellar light. A similar sequence forms the basis of all coronagraphic concepts, with the occulting mask replaced by the relevant coronagraphic mask.

A similar sequence forms the basis of all coronagraphic concepts, with the occulting mask replaced by the relevant coronagraphic mask.
The video linked here better explains how it works.

The design still had several problems, which included limited angular resolution due to diffraction caused by the occulting mask, high sensitivity towards telescope imperfections, diffraction rings present in the point spread function of the coronagraph and chromatic aberration increase. These led to the development of more advanced types of Coronagraphs like:

- Improved Lyot coronagraphs with amplitude masks
- Improved Lyot coronagraphs with phase masks
- Interferometric coronagraphs
- Optical vortex masks

The video linked above featured the method of using a deformable mirror to reduce atmospheric distortions of the wavefront through a constant feedback mechanism, this is called Adaptive Optics.

4.4.3 Infrared imaging

Observations in the infrared are facilitated by the simultaneous decrease in emission from the star and increased thermal emission from the planet, and by the implementation advantages of adaptive optics at longer wavelengths, which are the main reasons it is used often. However, there is a continuing debate about the relative merits of detecting and characterising Earth-like planets in the visible stellar light reflected by the planet, or in the thermal infrared.

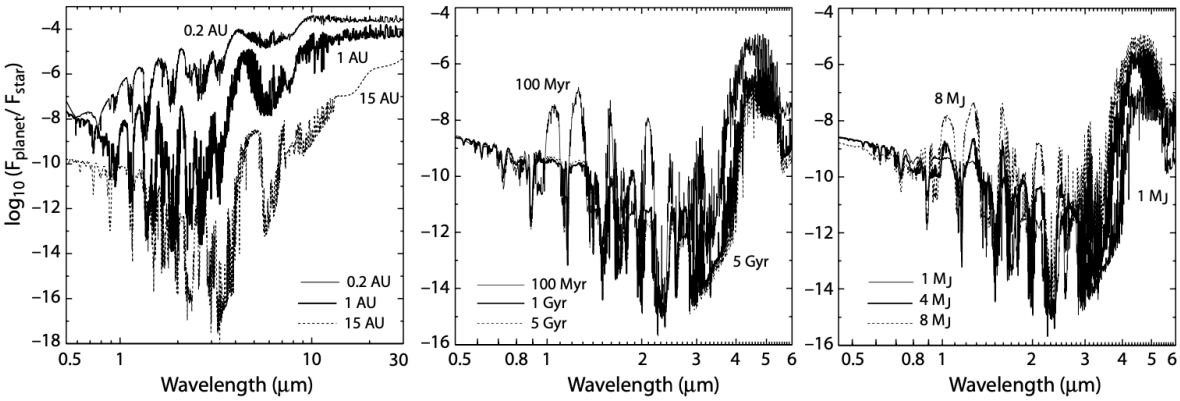

Figure 4.9: Predicted planet/star flux ratios versus wavelength. Models are for giant planets orbiting a G2V star of solar metallicity (phase-averaged, zero eccentricity, zero orbital inclination, effects of H_2O and NH_3 clouds included): (a) for a $1M_J$ planet with an age of 5 Gyr as a function of orbital distance. The flux ratio is dominated by reflection in the optical (Rayleigh scattering and clouds), and by emission in the infrared; the transition occurs between 0.8–3 μm depending on separation; (b) for a $1M_J$ planet at 4 AU as a function of age; (c) for a 5 Gyr planet at 4 AU as a function of planet mass (Perryman, 2011, p.150)

Here you can see the relatively large variation in the graph with orbital separation, and that infrared regions show higher SNR values.

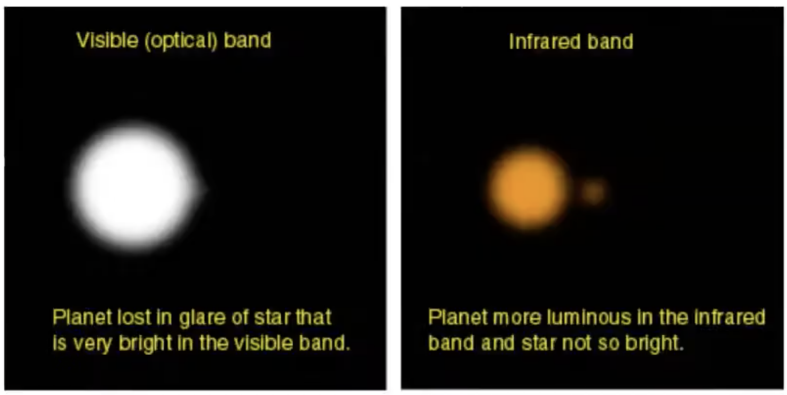

Figure 4.10: Visible vs Infrared imaging, Credit

In visible light, the typical method is to use coronagraphic methods with a single telescope or use an interferometric array (nulling interferometry- beams from multiple slightly offset telescopes are superimposed to create destructive interference in one part (the stellar region) and constructive in another (everything else)). Infrared imaging works differently and is used with the concept of a free flying interferometer.

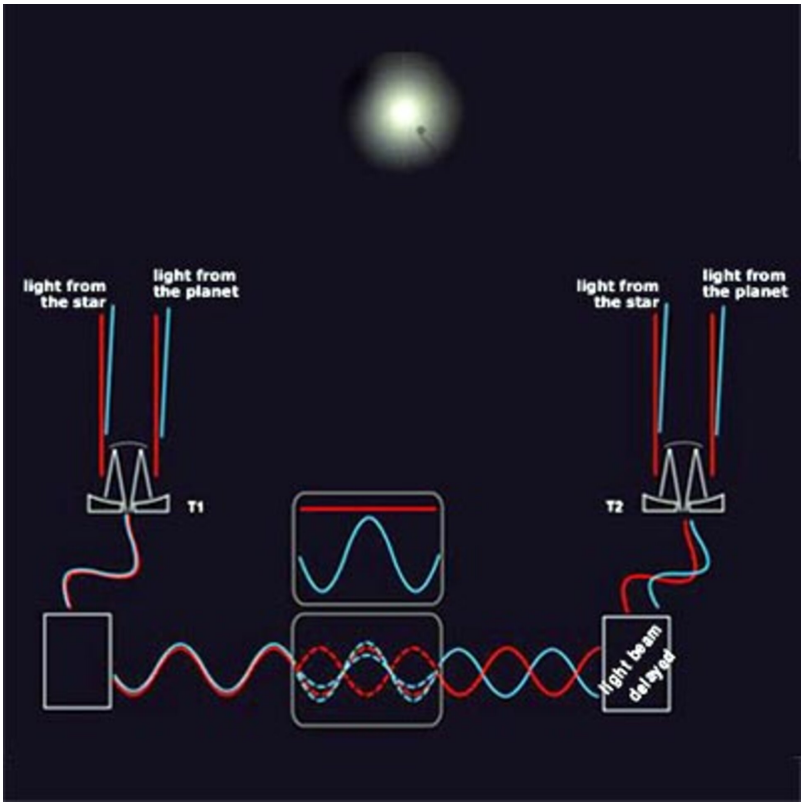

Figure 4.11: Nulling Interferometry

However, there are problems associated with infrared imaging as well:

- For a given angular resolution $1.22\lambda/D$, IR wavelengths require larger aperture mirrors
- At visible wavelengths the telescope does not contribute to the radiation background, meaning that the telescope can be operated at around 300 K, offering significant engineering advantages over a thermal infrared instrument which would need to be cooled to ∼40 K.
- In the thermal infrared, background radiation from solar system zodiacal light is a further complication.
- In the visible, spectral features and associated planetary diagnostics are more numerous than in the infrared
  - The light obtained contains spectral lines which are studied to learn about the properties of planets
  - Infrared also holds important information like the molecular bands of CH_4, CO_2 H_2O, and O_3 which have been considered particularly valuable diagnostics for the presence of life.

Although a visible light system could be significantly smaller than a comparable infrared interferometer, significant advances in optical mirror technology would be required.

4.5 Discoveries

Till now, over 200 planets have been discovered by this method, the first being 2M1207b, which in fact, orbits a brown dwarf and one of the most famous examples being HR8799, a roughly 30 million-year-old main-sequence star located 133.3 light-years away, around which 4 exoplanets were simultaneously imaged.

This field is expected to advance significantly with the development of advanced coronagraphic techniques, adaptive optics systems, and technology like starshades, but while that happens, you can enjoy this **literal** heavenly bodies posing for us:
https://en.wikipedia.org/wiki/List_of_directly_imaged_exoplanets

Gravitational Microlensing

5.1 Introduction

In general relativity, the presence of matter (energy density) distorts spacetime, and the path of electromagnetic radiation is deflected as a result. Under certain conditions, light rays from a distant background object (the source) are bent by the gravitational potential of a foreground object (the lens) to create images of the source which are distorted (and possibly multiple), and which may be highly focused and hence significantly amplified. This is called Gravitational Lensing (video).

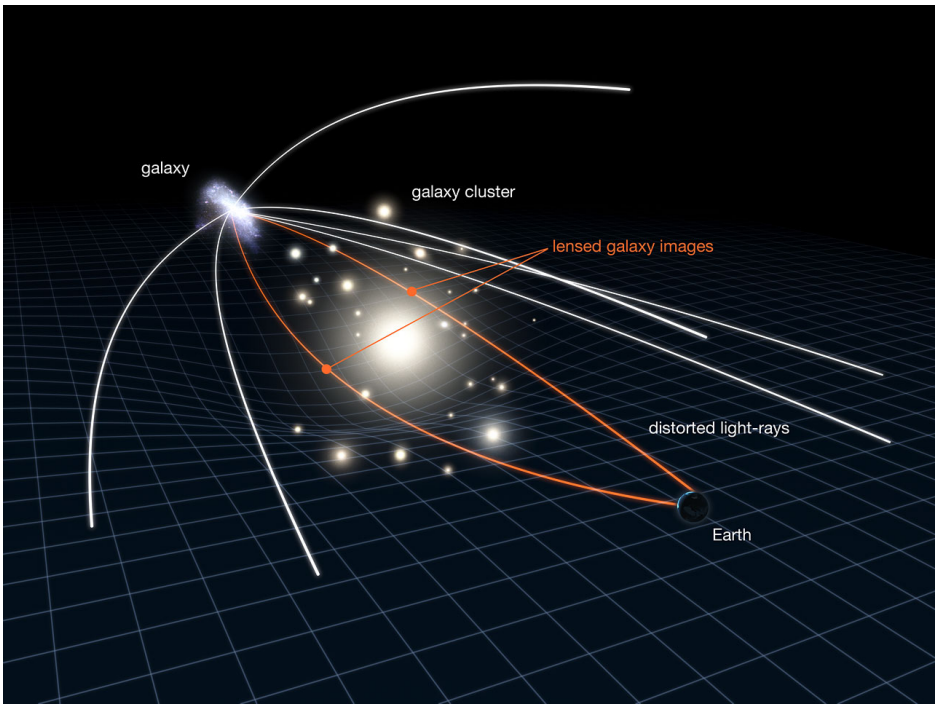

Figure 5.1: Gravitational lensing, Credit

It was first observed by Arthur Eddington, Frank Watson Dyson, and their collaborators in 1919 during a solar eclipse. The stars close to the sun, which could now be observed, appeared slightly out of position, showing that the light coming from them was bent by the sun's gravitational field, since then we've discovered some of the oldest galaxies, through lensing alone.

There are three main forms of gravitational lensing:

- In strong lensing, the lens is a large mass like a galaxy or a galaxy cluster, the geometry is favourable, and the deflection is comparatively large. The observer sees two or more separate images of the source.
  - Even a galaxy with a mass more than 100 billion times that of the Sun will produce multiple images separated by only a few arcseconds. Galaxy clusters can produce separations of several arcminutes.
- In weak lensing, the lens is a large mass (as above), but the geometry is less favourable. The image of the source is mildly distorted, with a tendency to smear into an arc centred on the lens centre: an effect known as shear. This means that the alignment, or stretch of the background objects appears non-random.
  - The light arriving from a population of distant galaxies is smeared similarly, leading to distortion along a specific direction, so this collective shear can be measured statistically even if the distortions of individual objects are too small to be identified directly.

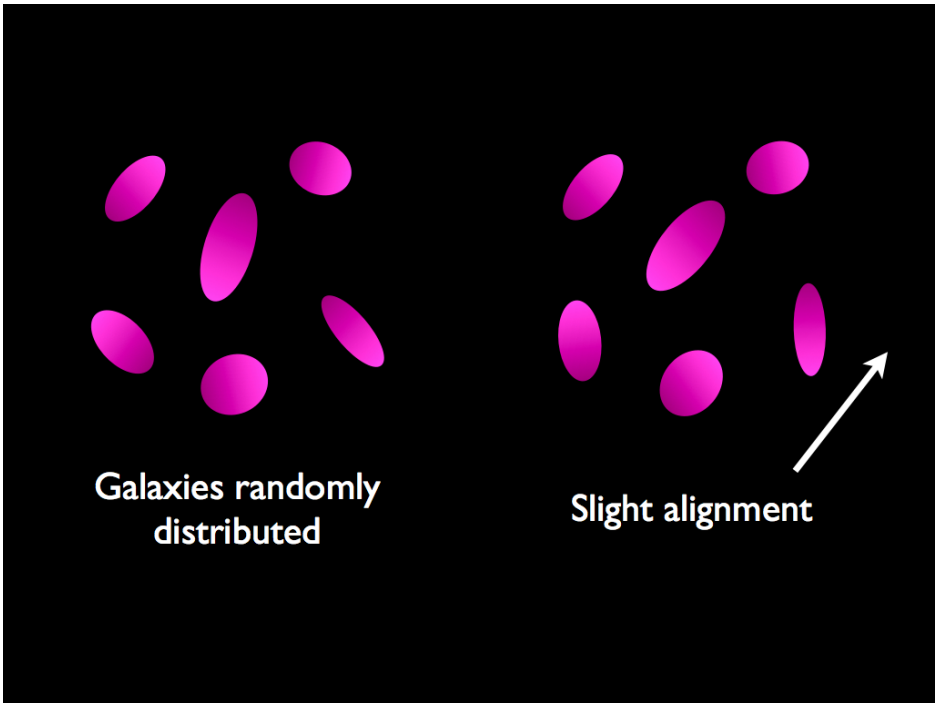

Figure 5.2: Weak Gravitational Lensing

- In microlensing, the lens is a small mass (usually a star), so that although the geometry is extremely favourable—source, lens and observer in a straight line—the deflection, distortion and multiple images caused by lensing cannot be resolved. Instead, the image of the the source appears to brighten for the duration of the lensing event (since source, lens and observer all have relatively proper motions, the alignment that creates the microlens is temporary) because the lens bends more light from the source towards us than it blocks (due to its small size).

On our quest to be the very best, like no one ever was (at finding exoplanets), the last one is what we're interested in. Take a look at these animations to get the gist of what happens
- https://www.youtube.com/watch?v=x1MQ0s0zqbw

5.2 Theory

5.2.1 Microlensing: Context

In Microlensing, discrete images of the source are unresolved at typical telescope resolutions. The term covers phenomena operating on galaxy scales (quasar microlensing) and on stellar mass scales and below (relevant for exoplanets). In the latter case, the primary lens is a single point mass of order $1M_{\odot}$, and the two images of a background source have a separation of order of only 1 mas, well below typical ground-based resolutions.

In the domain of interest for exoplanet detection, the exoplanet system (host star and planet) acts as a multiple lens, and a more distant star within the Galaxy acts as the probing source. The changing magnification of the sub-images due to the time-varying alignment geometry of the observer–host star–background source may lead to a significant intensity variation of the sum of the multiply lensed images over time scales of weeks. This changing intensity with time allows the event to be recognised as a microlensing event. Careful monitoring of the light curve as the alignment changes over several hours allows the additional lensing effects of an accompanying planet to be identified.

Such an alignment probability for any given source star in the Galaxy is so low that very large numbers of potential sources have to be monitored, frequently and simultaneously, to have any chance of observing even a single favourable configuration. The Galactic bulge region, with its high stellar surface density, is therefore the target monitoring region of choice. (For configurations of relevance, a typical source lies at a distance of $\sim$8 kpc. In the unlensed state, it is generally faint or even invisible, and to first order is considered as a point source of light). Microlensing most effectively probes lens systems some half way to the source, where the host star (and any accompanying planets) may also be invisible.

The light curve of the background star is the observational signature of microlensing, and encodes the geometry and mass distribution of the lens system.

5.2.2 Basics of Lensing

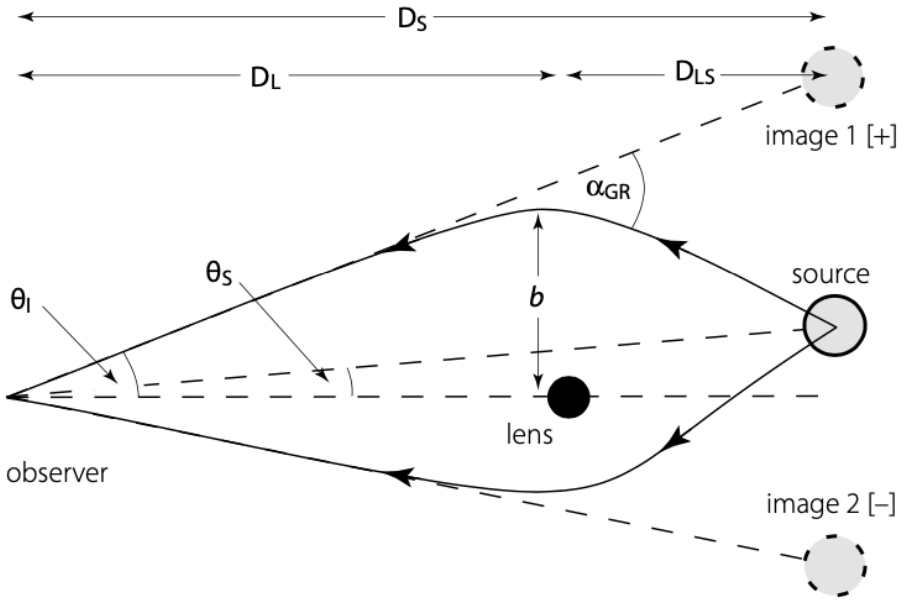

Figure 5.3: Schematic of a Lensing Event (Perryman, 2011, p.85)

The figure above is for a point mass lens ML at distance DL, offset by the small angle S from the direct line from observer to source. A light ray from the source, passing the lens at distance b, is deflected by an angle GR. An observer sees one image of the source displaced to angular position I = b/DL on the same side as the source, and a second image on the other.
For the geometry shown in Figure 5.1, the deflection angle GR for a light ray propagating past a lensing mass ML with impact parameter b is

$$\alpha_{GR} = \frac{4GM_L}{c^2 b} = \frac{2R_s}{b} \tag{5.1}$$

For $b >> R_S$, the Schwarzschild radius of the lens.

The images are what is visible to us, and the condition on α_{GR} such that the ray reaches the observer follows only from the trigonometry of the diagram. Using the usual approximations for small angles, $\alpha_{GR}, \theta_S, \theta_I$, in the image plane, we can see that:

$$\theta_S D_S = b\frac{D_S}{D_L} - \alpha_{GR} D_{LS} = b\frac{D_S}{D_L} - \frac{2R_S}{b} D_{LS} \tag{5.2}$$

Substituting $b = \theta_I D_L$, we get:

$$\theta_S = \theta_I - 2R_S \frac{D_{LS}}{D_L D_S}\frac{1}{\theta_I} \tag{5.3}$$

It is convenient to define a variable called the Einstein Radius (its significance will be clear in a moment), the angular form is given by

$$\theta_E = \left[2R_S \frac{D_{LS}}{D_L D_S}\right]^{1/2} \tag{5.4}$$

Equation (5.3) can then be written:

$$\theta_I^2 - \theta_S\theta_I - \theta_E = 0 \tag{5.5}$$

Which has 2 solutions:

$$\theta_{+,-} = \frac{1}{2}\left(\theta_S \pm \sqrt{\theta_S^2 + 4\theta_E^2}\right) \tag{5.6}$$

Hence, it is clear that 2 images are formed, one on either side of the lens (positive and negative solutions). In the hypothetical case of no offset, $\theta_S = 0$, the observer, lens and source are collinear and the images are rotationally symmetric about the line of sight to the lens, with angular distance from the lens θ_E

Brightening of the two images occurs because the flux from each is the product of the constant surface brightness of the source and the now enlarged solid angle subtended by the distorted image. The magnification for each image is given by the ratio of the image area to the source area:

$$A_\pm = \left|\frac{u_\pm}{u}\frac{du_\pm}{du}\right| \tag{5.7}$$

Which comes out to be:

$$A_\pm = \frac{1}{2}\left(\frac{u^2+2}{u\sqrt{u^2+4}} \pm 1\right) \tag{5.8}$$

Where

$$u = \frac{\theta_S}{\theta_E}, u_\pm = \frac{\theta_\pm}{\theta_E} \tag{5.9}$$

The following figure shows the formation of images, as the source moves on a linear trajectory:

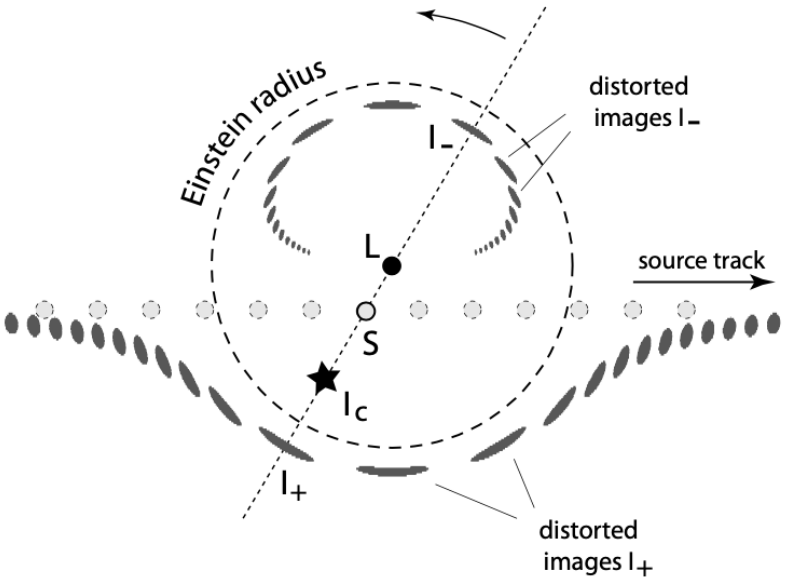

Figure 5.4: Schematic of Microlensing: $I_{\pm}$ - Image, I_C - Centroid, L - Lens, S - Source (Perryman, 2011, p.85)

for u –> 0, the case of $\theta_S = 0$, the magnification tends to infinity, and both images lie at the same angular separation, this results in the source being warped into a kind of ring, around the lens. The radius of this ring is, you guessed it, the Einstein radius.

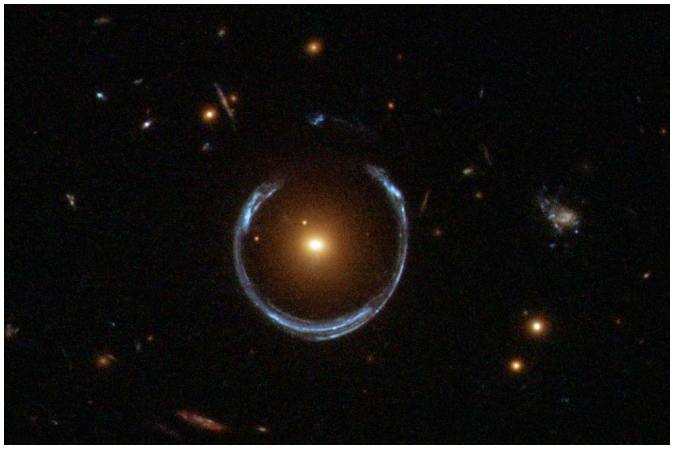

Figure 5.5: The Einstein Ring

5.2.3 Exoplanets from microlensing

As the lens passes in front of the source, the varying intensity for a single lens can be represented in the form of light curves as below, depending on how close they pass:

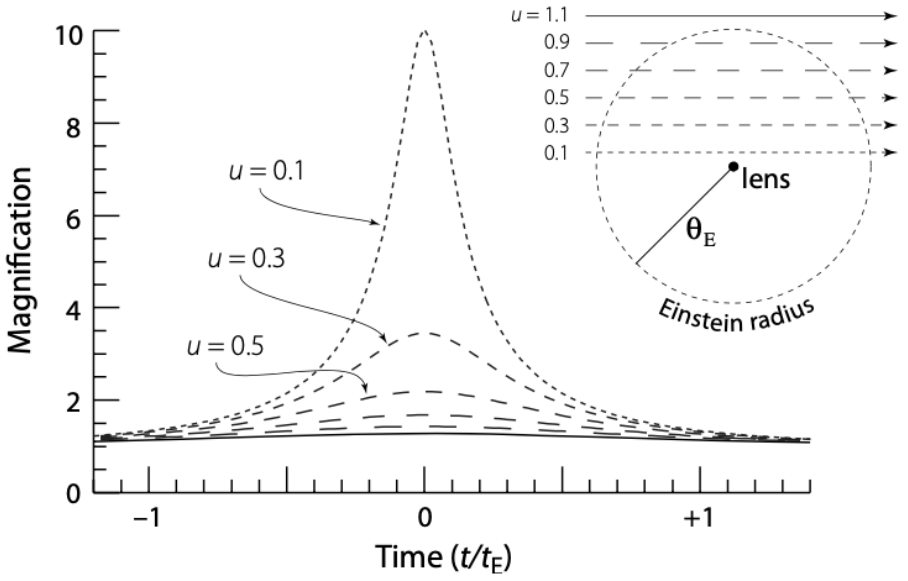

Figure 5.6: Single-Lens Light Curves, for different source trajectories in the top right (Perryman, 2011, p.86)

This is for a single lens system, where the only relevant parameter is t_E, the Einstein radius crossing time, in a binary lens, the second lens introduces variables of $q = M_P/M_\star$, projected separation a, and the angle of source trajectory, wrt the binary axis, α, which all contribute to a wide variety of light curves.

Compared to the smooth light curves of single-lens microlensing, the existence of a planet can result in additional short-duration peaks depending on how the source path crosses the lens projection.

The duration of planetary events typically scales with $q^{0.5}$, and lasts typically less than a day, compared with a typical primary lens event duration of 30–40 d. As q decreases, the peak signals become rarer and briefer: for Earth-mass planets, typical time scales are only 3–5 h.

Caustics and Critical curves

Caustics and Critical curves play an important role in determining the light curve shape.

Critical curves are the curves in the lens plane where the magnification of the source becomes infinite. They are caused by the alignment of the source, lens, and observer, leading to strong gravitational lensing.

Caustics are the corresponding curves in the source plane, mapping the regions where the magnification is significantly enhanced.

When you look at the bottom of a swimming pool under the sun, the rippling surfaces create lines, and patterns of light, similarly in a glass with water, the curves of light, and concentrations

of incoming rays. These are caustics on the image plane. They describe the function by which source positions viewed in the lens plane, are mapped to locations in the image plane.

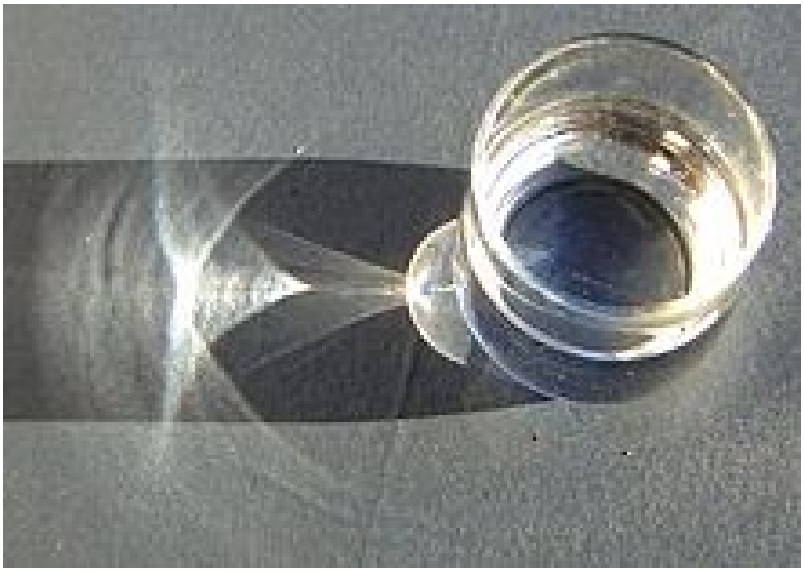

Figure 5.7: Caustics in everyday life

This video explains the workings of caustics in the context of lensing, in brief, if you're interested.

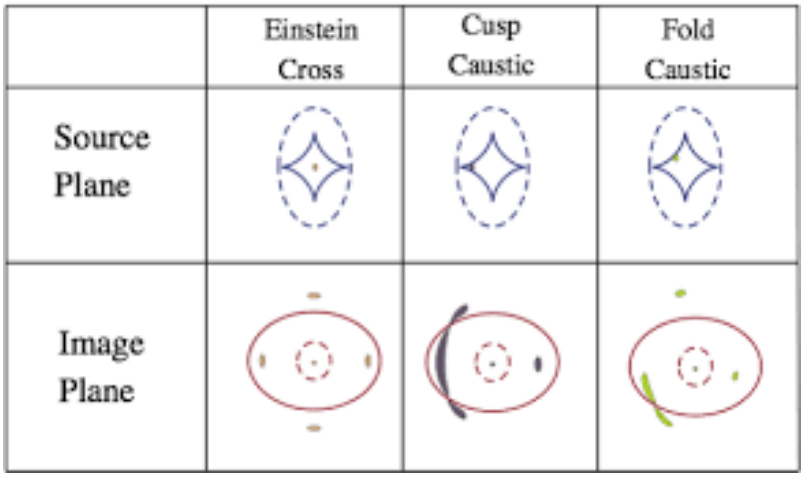

Figure 5.8: Images formed for various source positions, Credit

The caustics of binary lenses play a crucial role in the interpretation of exoplanet microlensing light curves. When the lens consists of two point-like objects, specifically a star and an orbiting planet, the caustic positions and shapes can be formulated in terms of the planet-to-star mass ratio q = Mp/M, and the angular star-planet separation d (in units of E). For arbitrary distances and mass ratios, the caustic structures are extended and complicated in shape, but for small values of q, and for d = 1, the picture is more straightforward.

Caustics and Critical curves are analogous to the centre of the lens, and the Einstein ring in the image plane respectively. The first is a point, line or curve of large magnification and the latter is where the image is stretched along.

If you're interested in the shapes of Caustics and where they come from, the research paper linked here can get you started.

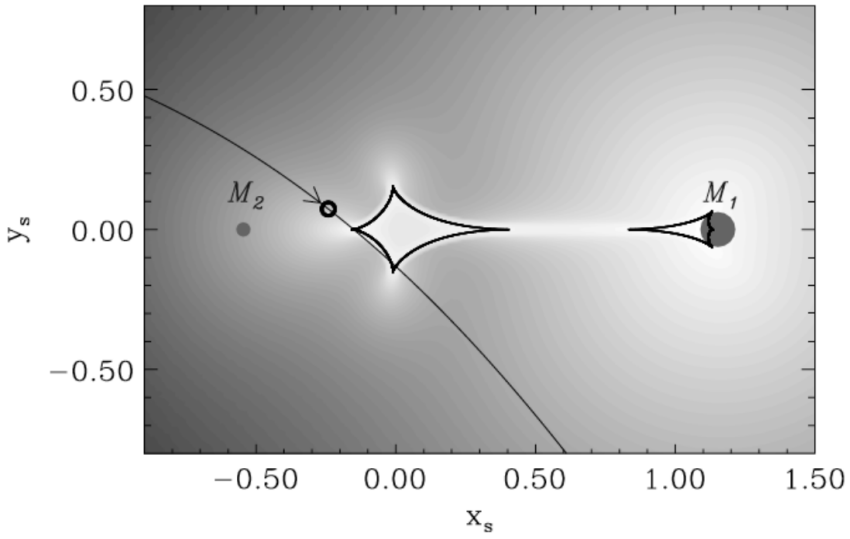

Figure 5.9: Caustics in a binary lens plane, Credit

As mentioned before, these determine the kind of light curves you'll see, and we can model these caustics so as to create a fit for the light curves observed.

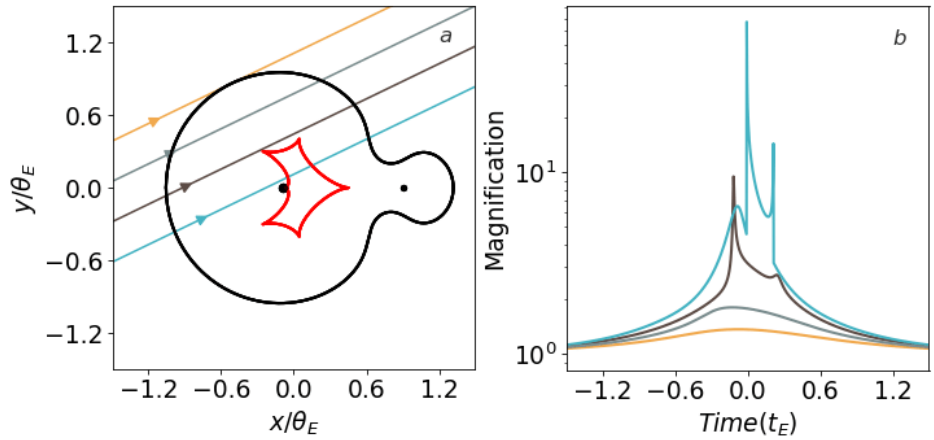

Figure 5.10: Example - Caustics, Critical Curves and Light Curves (Source trajectory marked with lines), Credit

The mathematics of binary lens systems is beyond the scope of this module, so we'll leave it at that. A few wonderful cases of this method can be found with a bunch of animations at http://spiff.rit.edu/classes/resceu/lectures/microlens/microlens.html :)

5.3 Discoveries

As of July 2023, there are over 60 exoplanets that have been discovered using gravitational microlensing. This method is particularly well-suited for finding very faint planets or that orbit very low-mass stars, due to the mass ratio factor playing a significant role.

A Major downside to this method is that microlensing events happen only once, for a given source, and may never happen again giving us no chance to confirm our hypothesis, Even then, planetary deviations in the light curves are short-lived, of order hours or days, and the most crucial features easily missed due to observational constraints. Nevertheless, current survey and follow-up programmes are now delivering significant numbers of planetary events.

Given suitably high monitoring frequency and high photometric accuracy, the strengths of this detection method, which will be further augmented if space-based measurements are carried out in the future, include its sensitivity to low-mass planets, in principle down to $M_{\oplus}$ and below, because of the nature of lensing itself, where low masses can also have significant effects. Rogue and dark planets can also be spotted.
Here are a few examples:

- OGLE-2005-BLG-390Lb: This was one of the first Earth-mass planets discovered using microlensing. It is roughly five times the mass of Earth and orbits a cool red dwarf star located about 21,500 light-years away in the constellation Scorpius.
- OGLE-2016-BLG-1195Lb: This planet was discovered in 2016 and is about 13,000 light-years away from Earth. It is a gas giant with a mass approximately 13 times that of Jupiter, making it one of the more massive planets discovered using microlensing.
- OGLE-2016-BLG-1190Lb: This is another intriguing find from the OGLE project. It is a rogue planet that does not appear to be orbiting any star. It is estimated to be around 1.9 times the mass of Jupiter and is located about 22,000 light-years away from Earth.

Astrometry

6.1 Introduction

Astrometry is the method that detects the motion of a star by making precise measurements of its position in the sky. This technique can be used to identify planets around a star by measuring tiny changes in the star's position as it wobbles around the centre of mass of the planetary system. Astrometry gives you the projection of the photo centre (The centre of light emission for a dispersed source) of the star on the plane of the celestial sphere, as the planet, or whatever the object be, orbits around it, allowing us to see the reflex motion of a star due to presence of a planet. Here's an animation to get an idea - https://exoplanets.nasa.gov/resources/2288/astrometry/

To actually get information from astrometric measurements, we need to measure the position **very** precisely, in fact, Astrometry was the very first method used to try and detect exoplanets, in the 19th century. However, instruments just weren't advanced enough to give reliable measurements.

The precision required to detect a planet orbiting a star using this technique is extremely difficult to achieve and hence it yields less results, although astrometry has been used to make follow-up observations for planets detected via other methods.

6.2 Theory

6.2.1 Measurement Principles and Accuracies

Our main goal is to spot perturbation in the orbit of a star's position, on top of the linear path of the system's barycentre (its proper motion) combined with the reflex motion (its parallax) resulting from the Earth's orbital motion around the Sun, and attempt to discern an orbiting planet from it.

Once we spot the perturbation, The path of a star orbiting the star–planet barycentre appears projected on the plane of the sky (for a face-on orbit, and a single planet) as an ellipse with angular semi-major axis α in length terms is given by (Perryman, 2011, p.61):

$$\alpha = \frac{M_p}{M_\star + M_p} a \simeq \frac{M_p}{M_\star} a \tag{6.1}$$

Where a is the **maximum** separation of the star and planet. This comes from the centre of mass system for a 2-body system, consisting of the Star and Planet.

In angular terms, hence α is given by:

$$\alpha = \left(\frac{M_p}{M_\star + M_p}\right)\left(\frac{a}{1AU}\right)\left(\frac{1pc}{d}\right) arcsec \tag{6.2}$$

This astrometric signature is observable for astrometric planet detection and is proportional to both Mp and a, and inversely to d. Astrometry is therefore particularly sensitive to long orbital periods (P $>$ 1 yr), applying equally to hot or rapidly rotating stars. The accuracy required to detect planets astrometrically is typically sub-mas (milliarcsec), although it would reach a few mas for planets of $M_P \sim 1 M_J$ orbiting nearby solar-mass stars (Why?). Obviously, this is ignoring multiple of the other motions of the star observed, but we'll get to that later.

The principle behind obtaining precise locations of a star, is by comparing the location to a reference frame, usually consisting of stars with well-defined locations (as the animation suggested), this is called Differential Astrometry.

The ideal accuracy of any imaging system is limited by unavoidable photon noise, which in this case is of the order of 10μas, which isn't as much as to worry about. Mainly as a result of atmospheric turbulence as shown before and differential chromatic refraction, however, even the best astrometric accuracies achieved on the ground currently fall short of this theoretical performance. Milliarcsec accuracies are considered impressive.

Space observatories like Gaia, where there is no atmosphere to worry about, are a different story, which reaches μas accuracies.

With μas accuracy available, effects like Light deflection, and Source motion (radial proper motion, perspective acceleration) become significant, even when these are accounted for, below 1 μas, stellar surface 'jitter' may pose a significant boundary, where stellar surface structure (star spots, plages, granulation, and non-radial oscillations) are likely to produce a difference in the photo centre measured and the actual stellar mass centre, which we ideally want to be the same.

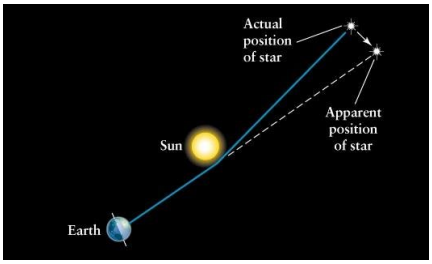

(a) Light deflection, Credit

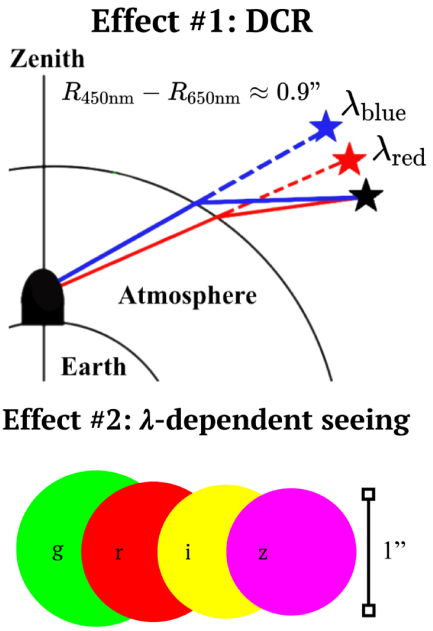

(b) Differential Chromatic Refraction, or Atmospheric Dispersion

Figure 6.1: sub-mas errors

All of these methods have reduced the significance of Astrometric claims of exoplanets in the past, but let's suppose we're able to measure the position without error, what data can we obtain from astrometric measurements?

6.2.2 Inferences

The motion of a star observed from Earth, would include the effects of proper motion as well as parallax due to the Earth's revolution, to produce something like this:

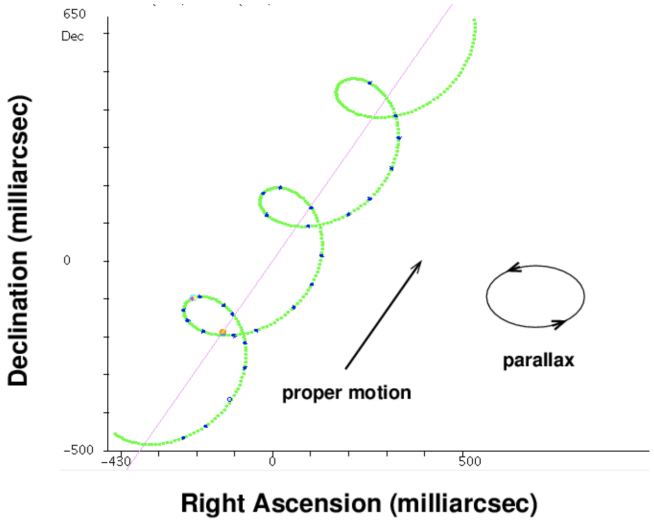

Figure 6.2: Movement of a star solely due to proper motion and parallax over 3 years, Credit

[Try and find the values for the proper motion and parallax using the information given] However, in the presence of an orbiting body, the star would wobble around this path, with the system barycentre travelling along the green path.

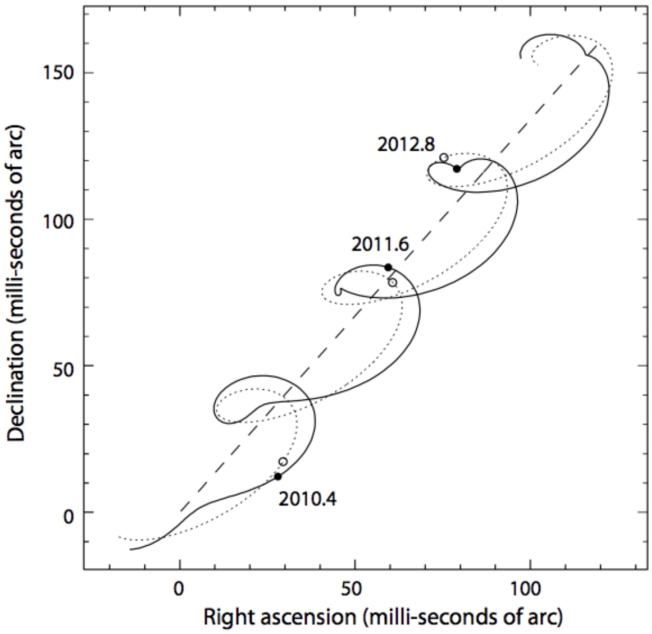

Figure 6.3: Movement of the same star measured by Hipparcos over 3 years (Perryman, 2011, p.62)

We must do a very good job of fitting and removing both these motions to get the residual orbital motion which is of use to us.

The cutest thing you can get is a Star orbiting the barycentre in a circle. Obviously, the planet isn't visible itself..

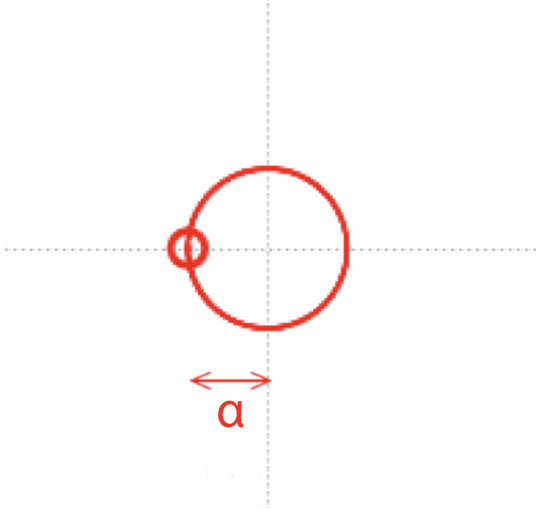

Figure 6.4: Simplest case of orbital motion observed of a star around the barycentre, Credit

Using equation (6.2) would be fruitless, as it has 2 unknowns, a and M_p. $M_\star$ can be **estimated**

using the luminosity and HR diagram, which is good enough (error$\sim$20%), or other methods.

Our measurements also involve time, and the orbital period is something which directly relates to the semi-major axis of the orbit according to the very famous Kepler's third law.

$$P^2 = \frac{4\pi^2}{G(M_p + M_\star)} a^3 \tag{6.3}$$

where G is the universal gravitational constant, P is the period, and a is still the maximum distance between the star and planet.

Let $M_p = m$ & $M_\star = M$.

If we consider the ratio $m/M = \gamma$, the equation can be changed to:

$$P^2 = \frac{4\pi^2}{GM(1+\gamma)} a^3 \tag{6.4}$$

From eqn (6.1):

$$P^2 = \frac{4\pi^2}{GM(1+\gamma)} \alpha^3 \left(1 + \frac{1}{\gamma}\right)^3 \tag{6.5}$$

Rearranging:

$$\frac{\left(1 + \frac{1}{\gamma}\right)^3}{(1+\gamma)} = \frac{GMP^2}{4\pi^2\alpha^3} \tag{6.6}$$

Observe the graph of the LHS function vs γ, what do you notice?

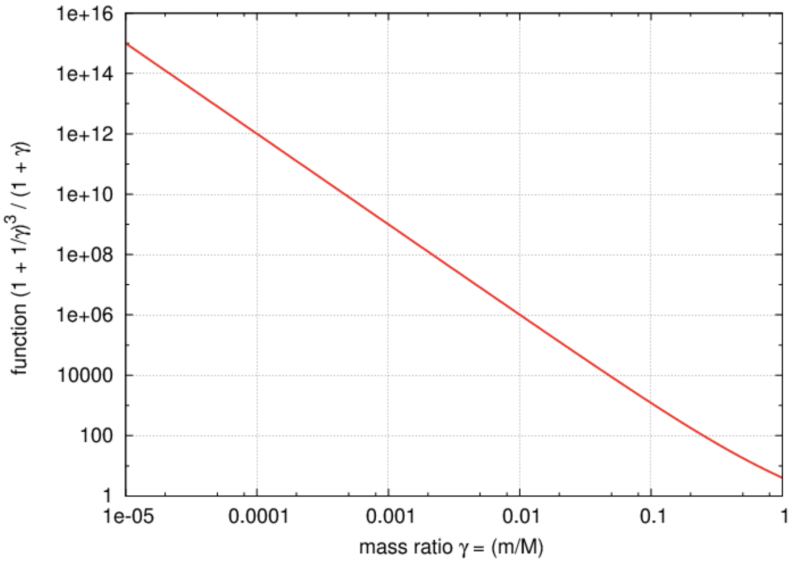

Figure 6.5: Credit

It shows that for $0 < \gamma \leq 1$, we can obtain a unique γ, and hence, unique planet mass!

Other than the complication of proper motion and parallax mentioned, the only other complication in our method is probably orbital inclination. Whenever we look at an orbit, there is no guarantee it is face-on, as a result, as seen in Pulsar Timings and Radial Velocity methods, we are only able to put a lower limit on masses determined, as true planet mass $m \sin i \geq m_{obs}$.

However astrometric methods can discern orbital inclination, which allows them to be applied to a far more variety of stars than the other two, and provide supporting data for other follow-up methods. How?
Let us take the case of a plain elliptical orbit observed, if we look at the orbit as an elliptical curve, we don't know if we're looking at another ellipse, tilted at some angle (which makes another ellipse) or a face on orbit. The secret to finding out is **time**.

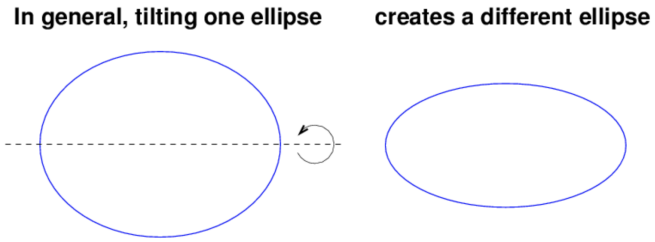

Figure 6.6: A fact to note, Credit

Let's look at 2 elliptical orbits, of roughly the same eccentricity when viewed from a point, with the position of the body measured at equal intervals of time, and not continuous.

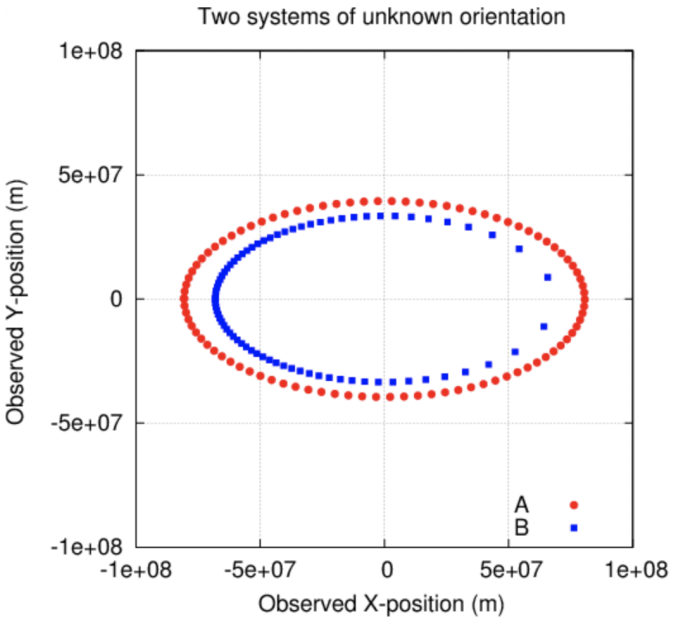

Figure 6.7: Credit

Now here are the same ellipses, face-on:

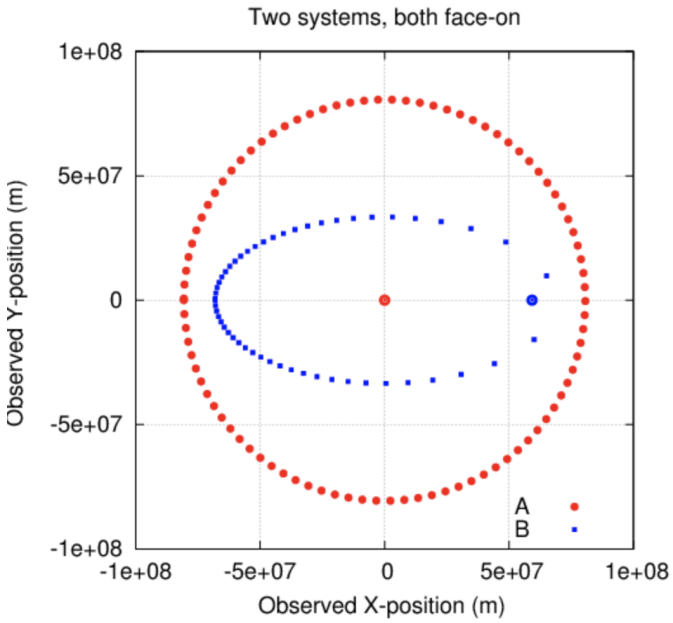

Figure 6.8: Credit

See the difference? You can tell the speed is greater for the blue curve towards the right. However, there is a reason face-on orbits are unique, all our equations of gravitation apply solely in that viewing frame unless we count inclination for the others. So, To find the inclination, we first take our elliptical orbit and its foci, one of these foci will be the orbital focus.

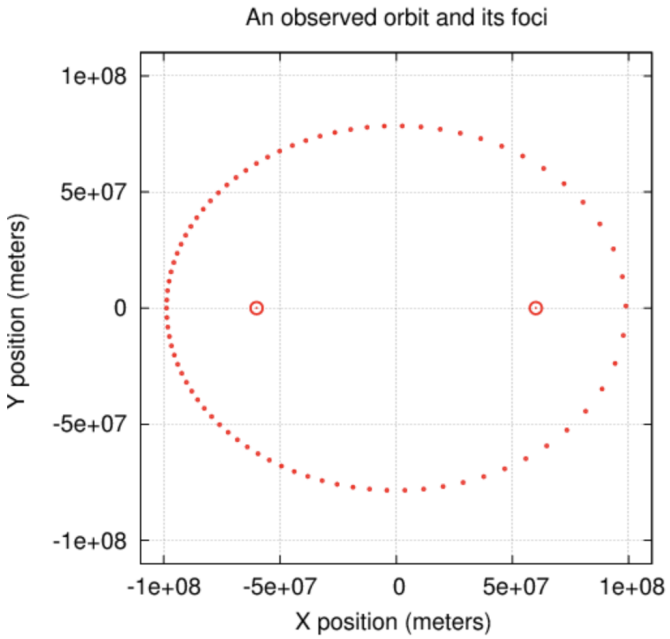

Figure 6.9: Credit

Kepler's Second Law, tells us that in equal amounts of time, equal areas are swept out by the orbiting body in the orbital plane :), Taking triangles formed by consecutively sampled positions and foci:

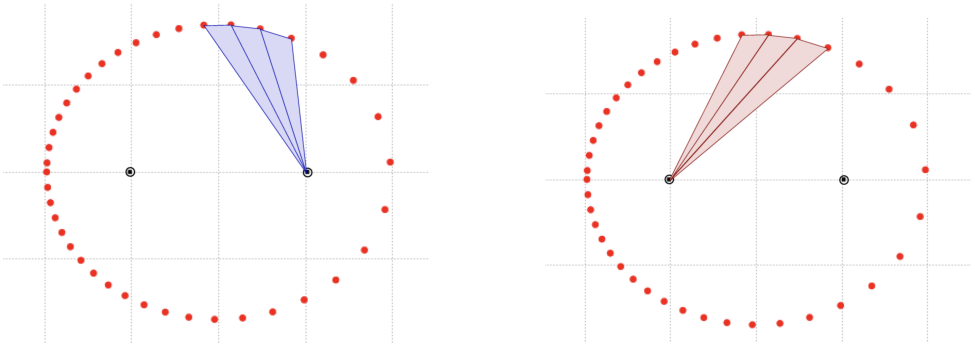

(a) (b)

Figure 6.10: Credit

Now if we compute the area swept out for each focus and plot it with time, we get:

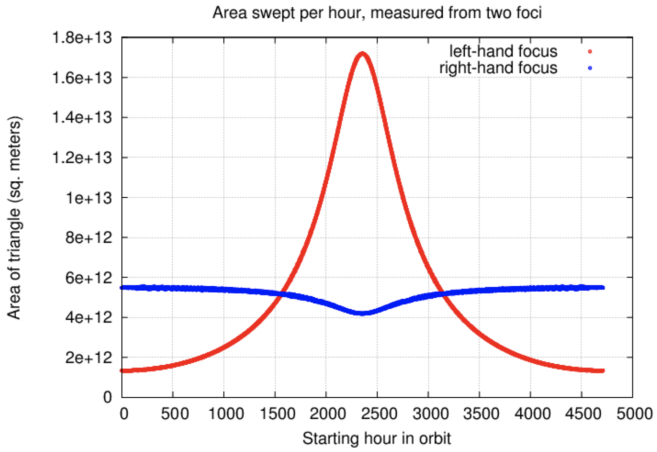

Figure 6.11: Credit

We'd expect one of the graphs to be a flat line, since neither is, you can be certain you're seeing the orbit at an angle :)

The blue graph certainly looks to be closer to the orbital focus, which checks out with the higher speed experienced on the corresponding side (what does this mean?), we still don't know the angle of inclination, but one thing we can do is de-project the ellipse through a range of possible angles, and do the same thing for all of them:

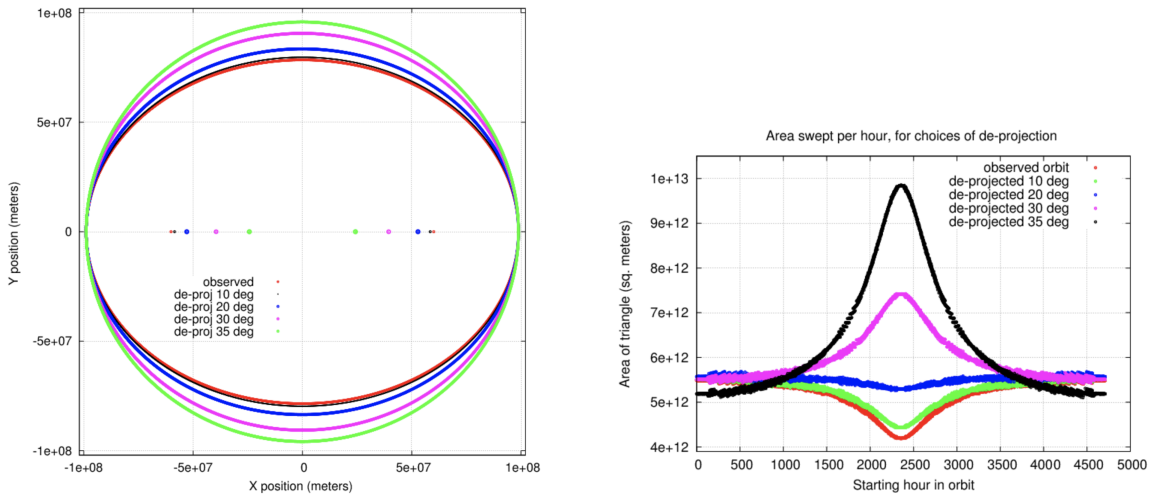

(a) (b)

Figure 6.12: Credit

Computers can do multiple tests and find the ideal fit by hit and trial.

What might it look like when a planet has multiple planets orbiting it?

The dynamical effect of multiple planets contributes to the total astrometric signature in the same way as the Sun's path over decades reflects the combined gravitational effects of all solar system objects. Here are some examples of the complex star paths in their orbit plane that result from the linear superposition of the reflex motions due to the orbiting of each individual planet around that star-planet barycentre.

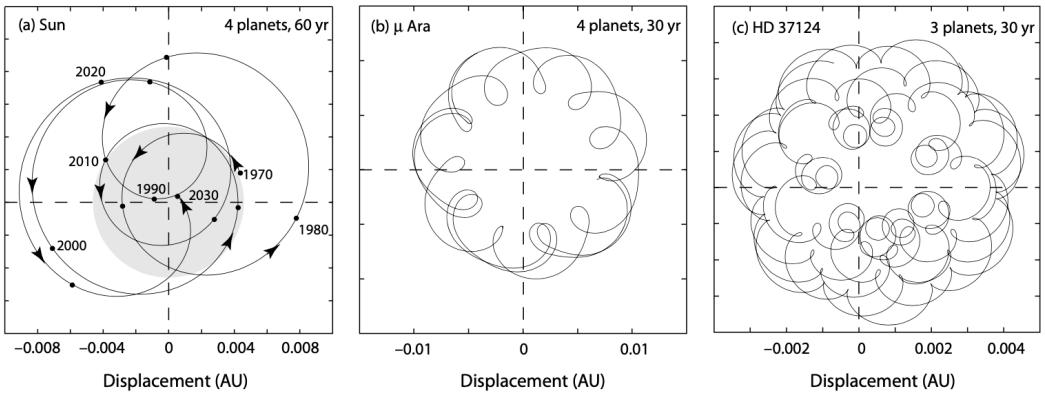

Figure 6.13: (a) Path of the sun's motion around the Solar System barycentre in the ecliptic planet, with the Solar diameter shown in grey for comparison. (b-c): The same motion for other stars measured through astrometry (Perryman, 2011, p.66)

These patterns have been called "Planet Mandalas". In a simplistic picture, as for orbit reconstruction in the case of radial velocity observations, each planet would have its own orbital

frequency, and Fourier analysis of the total signal would reveal the various planets. But that is a specialist's job, not ours.

6.3 Discoveries

Astrometry has had a rather tragic past. So far, through astrometry, we've been able to confirm a whopping 19 exoplanets (out of 5000+).
The difficulties involved with greater and greater precisions, along with the complexity of analysing and confirming exoplanets, from astrometric measurements, and the historically low accuracies and refuted claims, have slowed down.

Astrometry, however, it is the longest-standing method to date, we hope to see more results with the precision provided by spacecraft like Hipparcos and Gaia as well as development of methods to combat accuracy barriers and improve standards.

Gaia is a space observatory, launched by the European Space Agency (ESA) in 2013, A global space astrometry mission expected to operate till 2025. Gaia is building the largest, most precise three-dimensional map of our Galaxy by surveying nearly two billion objects, and we expect to detect more exoplanets through the astrometric data it provides, as well as Hipparcos, another mission by ESA.

Figure 6.14: The Gaia Observatory

Astrometry has had major success in detecting Massive gas giants, especially those in wide orbits (due to the large astrometric signature they cause) and Brown Dwarfs (Objects midway between gas giants and stars mass-wise).

Transits

7.1 Introduction

The study of exoplanets through Transits is the most successful method, mainly because of the successes of the Kepler and TESS NASA missions.

A transit (or astronomical transit) is a phenomenon when a celestial body passes directly between a larger body and the observer. As viewed from a particular point, the transiting body appears to move across the face of the larger body, covering a small portion of it.

When it comes to exoplanets, transits look nothing like the Transit of Venus, because we can't see a faraway star from limb to limb (end to end). So what do we see? As the transiting body passes in front of the larger light source, there is a drop in the brightness or flux received from the star due to the occulting. We see this in the form of transit light curves.

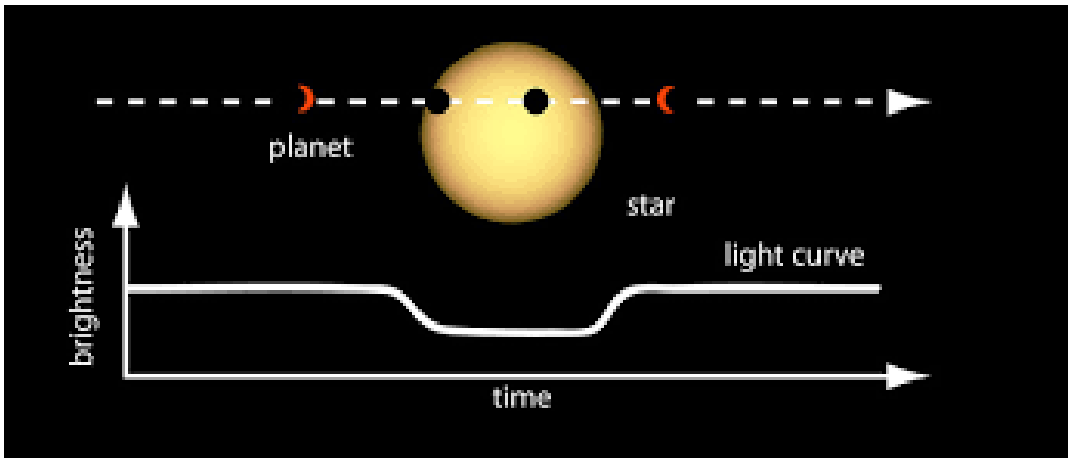

Figure 7.1: Transit light curve

Given a suitable alignment geometry, light from the host star is attenuated by the transit of a planet across its disk, with the effect repeating at the orbital period. This animation should give you an idea - https://exoplanets.nasa.gov/resources/2283/transit-method-single-planet/

7.2 Theory

Since we'll be talking about orbits, let us establish some terms we'll be using:

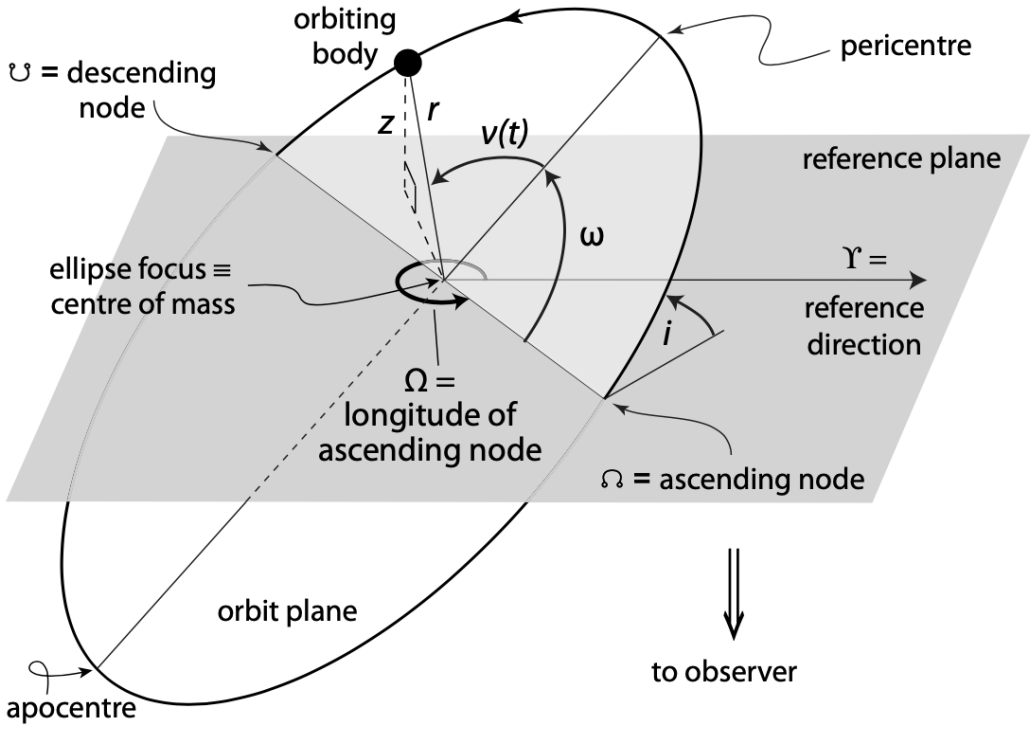

Figure 7.2: A 3-dimensional Keplerian Orbit (Perryman, 2011, p.10)

A Keplerian orbit (as shown) in three dimensions is described by seven parameters: $e, a, P, t_p, i, \Omega, \omega$

- e is the eccentricity of the orbit
- a is the semi-major axis of the orbit
- P is the Period, which is related to Kepler's 3rd law as
- t_p corresponds to the position of the object along its orbit at a particular reference time, generally with respect to a particular time when the object passes the pericentre.
- The three angles (i, Ω, ω) represent the projection of the true orbit into the observed (apparent) orbit
  - i specifies the orbit inclination with respect to the reference plane.
  - Ω specifies the longitude of the ascending node, it is the node where the measured object moves away from the observer through the plane of reference.
  - ω specifies the argument of pericentre, being the angular coordinate of the object's pericentre (point of closest approach) relative to its ascending node, measured in the orbital plane and the direction of motion. (taken 0 for a circular orbit $\rightarrow t_p$ is then wrt nodal passage).

v(t), or f(t), called a true anomaly, is the angle between the direction of pericentre and the current direction of the object at time t, measured wrt t_p, it is the angle normally used to characterise the orbit.

7.2.1 Transit Probability

To observe a Transit, you need specific orientations of the orbit you're viewing, a face on orbit doesn't transit, while an edge on one does.
The probability for a given star, with an orbiting planet that you'll be able to witness a transit at some time in its life in that orientation, is written as:

$$p_{tr} = 0.0045 \left(\frac{AU}{a}\right) \left(\frac{R_\star + R_p}{R_\odot}\right) \left[\frac{1 + e\cos(\pi/2 - \omega)}{1 - e^2}\right] \tag{7.1}$$

This comes from the area of the celestial sphere onto which the transit is projected.

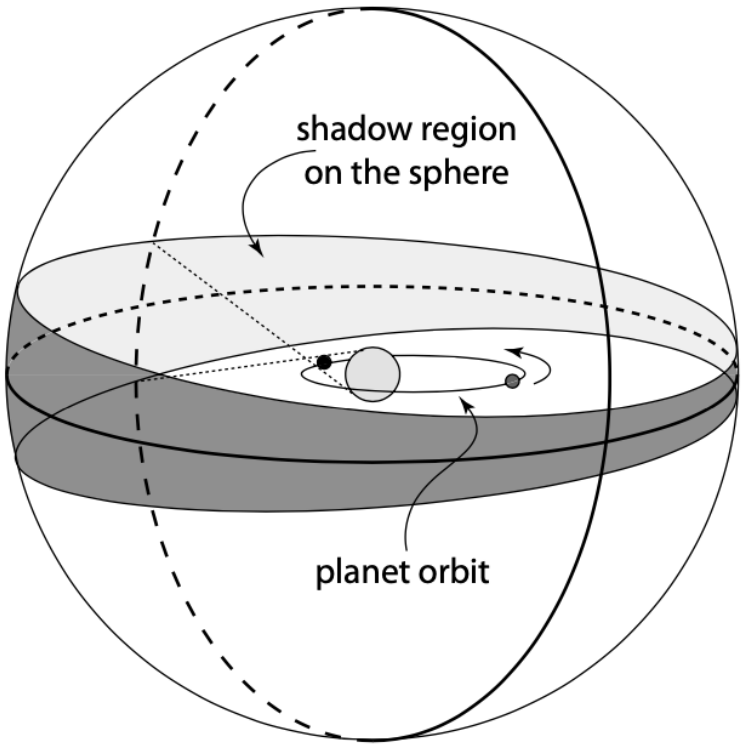

Figure 7.3: Transit "shadow" (Perryman, 2011, p.122)

Clearly, the fraction of the angle in which the transit can be observed is a function of the true anomaly v(t), integrating over all v(t) we get the average probability in (7.1).

For a circular orbit, e tends to 0, thus the fraction of the projected angle is constant and you

can see once you calculate the fraction of the small angle projected, (proportional to $(R_\star + R_p)/a$), the formula is pretty straightforward. The effect of eccentricity and argument of pericentre is seen as a result of integration.

This probability, clearly, is extremely small ($a >> (R_\star + R_p)$). It is also independent of star distance, but the corresponding photometric accuracy decreases.

The increasing majority of transiting planets are being found from dedicated wide-angle searches. Since there is little to indicate a priori which stars may have planets, which of those that do might be oriented favourably for a transit to be observed, and when or how frequently such transits may occur, surveys simply monitor large numbers of stars, simultaneously and for long periods of time, searching for the tiny periodic drops in intensity that might be due to transiting planets. It may take multiple years to confirm transiting exoplanets.

The effect being sought is also small: a planet with $R \sim R_J$ transiting a star of $1R_\odot$ results in a drop of the star flux of $(\Delta F/F) \simeq 1.1 \times 10^{-2}$, or around 0.01 mag. For planets of Earth or Mars radius, $\Delta F \simeq 8.4 \times 10^{-5}$ and 3×10^{-5} respectively. Depths of up to 7% might occur for M dwarfs.

Ground-based searches are able to discover transits with depths up to about $(\Delta F/F) \simeq 1\%$, revealing gas-giant planets around stars frequently bright enough for radial-velocity confirmation and mass measurements with 2m-class telescopes, or for study of their atmospheric transmission and emission spectra from space-based observations. Surveys from space, beyond the effects of atmospheric seeing and scintillation, are discovering planets with transit depths of a few times, 10^{-4} extending detectable exoplanet masses down to just a few $M_\oplus$.

Once we do observe a transit, It obviously won't result in a clean curve as shown earlier. Why not, and what are our limits?

7.2.2 Measurements, Error and Limits

Limitations from the ground: Nearby exoplanet host stars are typically comparatively bright, and telescope apertures can be very large. For surveys of the brightest stars, the contribution of photon noise to photometric transit measurements is accordingly generally negligible. Limitations on the smallest transit depths ΔF, and hence the smallest planet masses arise, instead, from a combination of atmospheric transparency variations, atmospheric scintillation noise, and detector granularity.

Have a look at the example of HD209458, the very first confirmed using transit, obviously we've done a good job at reducing error for these kinds of measurements since then, but this is to give an idea of the scales of error from Earth and space

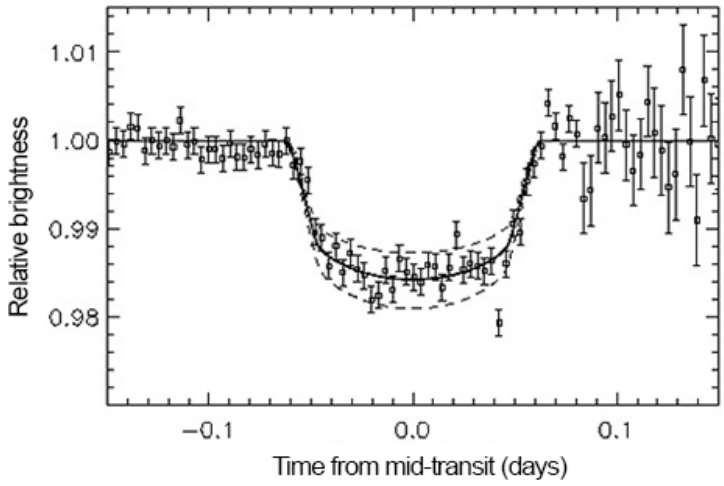

Figure 7.4: HD209458 Transit Light Curve (ground), Credit

Limitations from space: The fundamental limits on high-accuracy time-series transit photometry, obtained above the Earth's atmosphere, are imposed by the presence of stellar surface structure (star spots, plages, granulation, and non-radial oscillations), which are strong functions of spectral type. It is the same surface structure which sets limits on achievable radial velocity and astrometric accuracies. Now here's the transit for the same planet, observed from space:

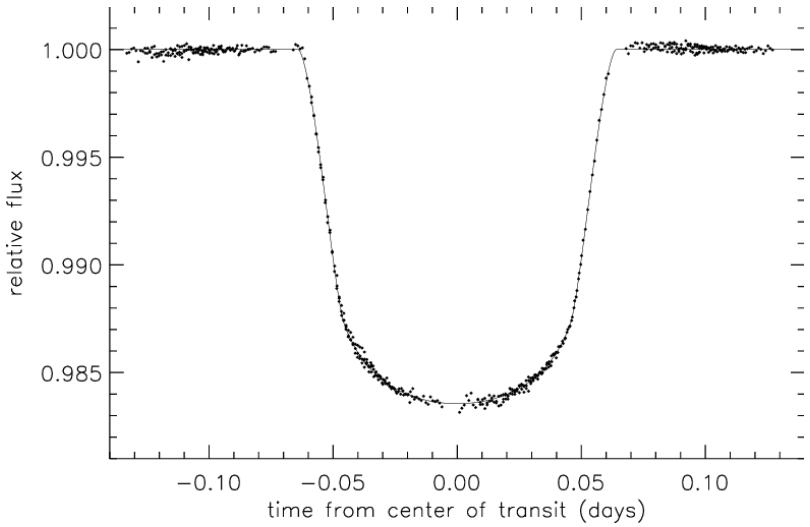

Figure 7.5: HD209458 Transit Light Curve (space), Credit

Notwithstanding the error bars, there is a clear win for space when it comes to precision. This doesn't belittle the number of successful discoveries from ground observatories, in fact, transits can be observed using telescopes in one's backyard. However, when it comes to smaller transits less than a few % drop, it becomes difficult.

Two of the most popular missions that contributed to Transit exoplanet detection were the Kepler Mission, launched in 2009, which had one of its jobs to survey one and study planet transits, as opposed to the TESS mission, which is still in use today and has wider coverage.

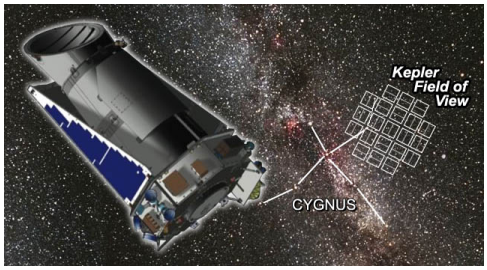

(a) Kepler Mission

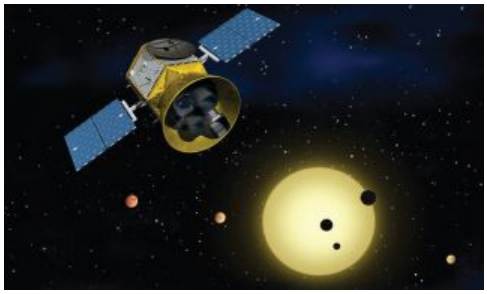

(b) TESS Mission

Figure 7.6: Exoplanet Discovery Missions

After measurements, theoretical light curves can be generated to create a best fit. In practice, Including the effects of stellar limb darkening, light reflected from the planet, blending due to background objects, and effects due to orbit eccentricity and other higher-order terms, make the problem a challenging one, yet rich in the physical information that the transit light curves convey. An important factor while modelling systems for theoretical light curves is Limb darkening:

7.2.3 Limb Darkening

When you look at a light curve of a transit, you may expect to see a box-like structure, with sharp drops at the edges, but if you look at a transit at different wavelengths, you'll see that its shape curves slightly. The figure below shows the transit of a planet around the star HD 209458 at wavelengths ranging from about 3000 Angstroms (purple, at the bottom) to about 10000 Angstroms (red, at the top).

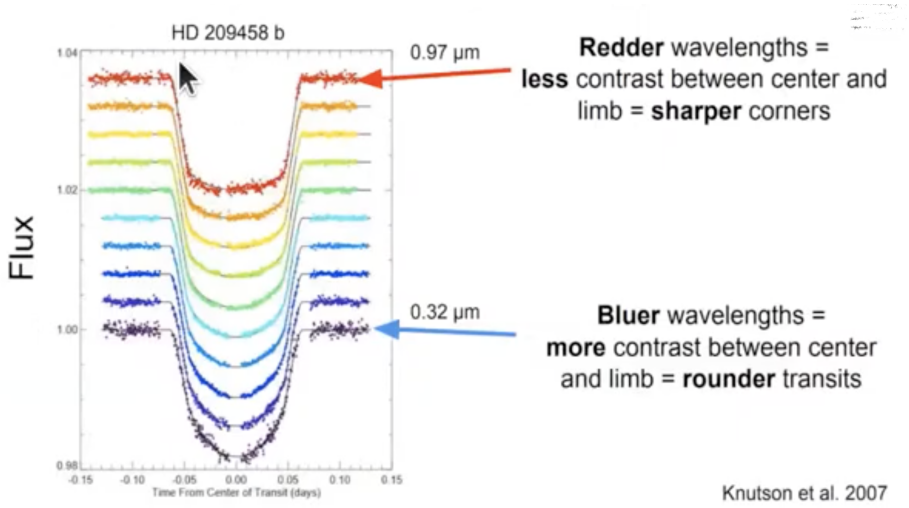

Figure 7.7: Effects of limb darkening on transmission spectrum

You might have noticed, that for shorter wavelengths, other than the obvious decrease in overall intensity emitted, the dip isn't as "sharp" as it is for larger wavelengths.

When you look at a star in the middle, the light you're seeing is from a deeper part of the star which emits higher energy light. This part of the star is called the **photosphere**, and it is the deepest part of the star which is still transparent to certain visible photons and as you move outwards, the peripheral emissions of the star comprise larger wavelengths in a higher percentage, the outer layers of the sun radiate lower energy light, thus the dropoff in the intensity of higher frequency light is smoother as you go outwards, hence, as the transiting planet blocks this wavelength at the "limb" (periphery), it doesn't lead to as sharp a drop as red light.

One important feature of limb darkening is that it depends on the wavelength at which one observes: shorter wavelengths lead to stronger limb darkening, because of the stronger gradient in emitted radiation between the inner and outer layers of the sun.
The dip in the light created by a transit shows us a sort of mirror image of the surface brightness of the star: the dip is deeper where the surface is brighter.

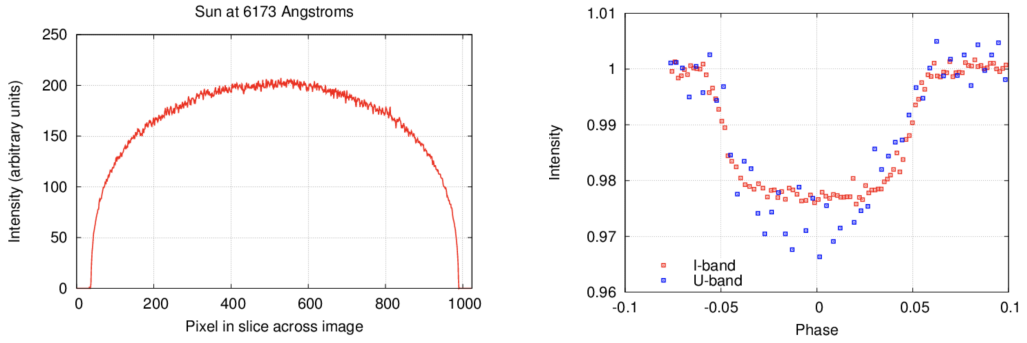

(a) Kepler Mission (b) TESS Mission

Figure 7.8: Limb darkening and transit samples, Credit

Once we obtain a light curve, what do we do with this information, and what can we learn?

7.2.4 Transit Light Curves

Aside from detection, there are a number of things that can be inferred from the properties of the transit light curve:

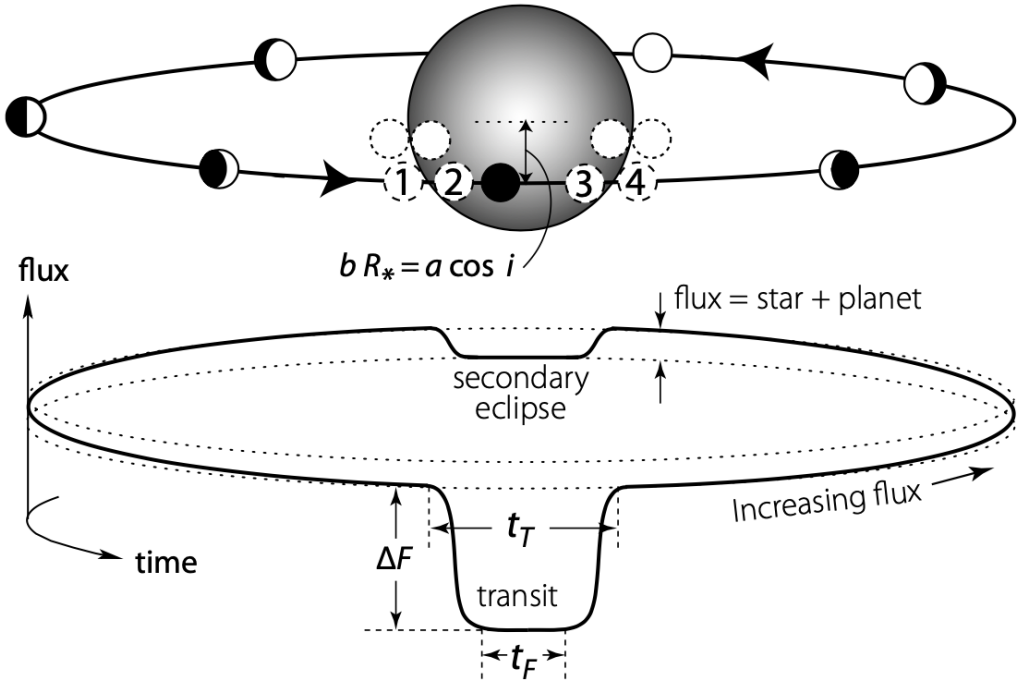

Figure 7.9: Transit Schematic, (Perryman, 2011, p.117)

There are four principle observables which characterise the duration and profile of the primary transit: the period P, the transit depth ΔF, the interval between the first and fourth contacts t_T (Total Transit Duration) and the interval between the second and third contacts t_F.

From these, three geometrical equations together describe the principle features of the transit light curve (Seager & Mallén-Ornelas, 2003, eqn 1-3):

$$\Delta F \simeq \left(\frac{R_p}{R_\star}\right)^2 \tag{7.2}$$

$$\sin\left(t_T \pi / P\right) = \frac{R_\star}{a}\left\{\frac{\left[1+\left(R_p/R_\star\right)\right]^2 - \left[\left(a/R_\star\right)\cos i\right]^2}{1-\cos^2 i}\right\}^{1/2} \tag{7.3}$$

$$\frac{\sin\left(t_F \pi / P\right)}{\sin\left(t_T \pi / P\right)} = \frac{\left\{\left[1-\left(R_p/R_\star\right)\right]^2 - \left[\left(a/R_\star\right)\cos i\right]^2\right\}^{1/2}}{\left\{\left[1+\left(R_p/R_\star\right)\right]^2 - \left[\left(a/R_\star\right)\cos i\right]^2\right\}^{1/2}} \tag{7.4}$$

The first follows from the ratio of the areas of the projected disks of the planet and star. The total transit time follows from the fraction of the orbital period P during which the projected distance between the centres of the star and planet is less than the sum of their radii. The formula for t_F is derived similarly.

Using these formulae, coupled with Kepler's 3rd law, many properties of the star and planet can be estimated, such as stellar and planet density, inclination and even planet surface gravity! When combined with data from other observation techniques, such as radial velocity measurements or spectroscopy, additional details about the exoplanet's composition, atmosphere, and potential habitability can be inferred.

Here's a transit simulation to demonstrate how the observations are made:
https://astro.unl.edu/naap/esp/animations/transitSimulator.html

7.3 Discoveries

The transit method has been one of the biggest contributors to exoplanet discovery, giving us around 4000 of them to catalogue. As the probability suggests, it has been better at detecting larger planets orbiting close to their stars, a very interesting class of exoplanets called **Hot Jupiters**. Here are some interesting planets that have been caught transiting:

- Kepler-186f: This exoplanet, discovered by Kepler, is notable because it is considered the first Earth-sized planet orbiting within the habitable zone of its star.
- TRAPPIST-1 System: The TRAPPIST-1 system, located about 40 light-years away in the constellation Aquarius, gained significant attention due to the discovery of seven Earth-sized planets orbiting a small, dim star. Three of these planets are within the star's habitable zone, making them potentially suitable for liquid water and raising intriguing possibilities. In fact, transits aren't always by single planets, this is a wonderful example:

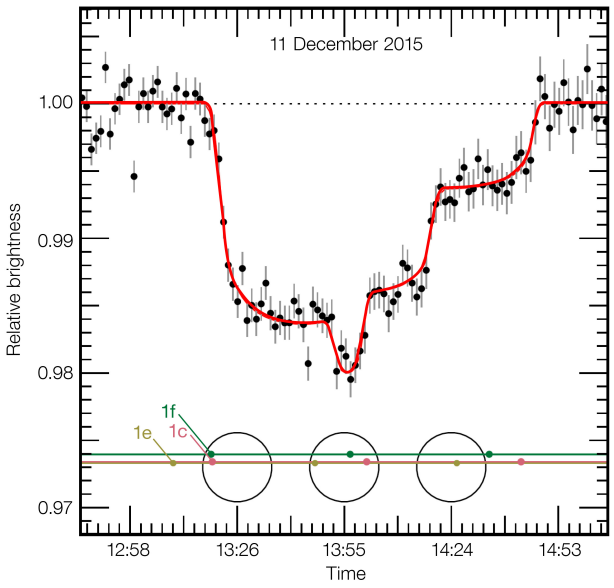

Figure 7.10: Trappist 1 light curve, Credit

- WASP-12b: This exoplanet, located about 1,400 light-years away in the constellation Auriga, is particularly interesting because it is one of the hottest known exoplanets. It orbits extremely close to its host star and exhibits significant atmospheric expansion and tidal interactions.

Radial Velocity

8.1 Introduction

In a planetary system, the star holds a majority of the mass, thus, the centre of mass sits very close to the sun, but not exactly at the centre, a very important precursor to the principle of this method.

As the Star and planet go around the COM, at some instance in the orbit, it would be coming towards us along the line of sight of the earth, and at some point, it's going away. This wobble is obviously not visible from where we are, (If it is, and the effects aren't even that large.
A planet orbiting around a Sun-like star, with the mass of Jupiter and an orbital period of 1 earth year, in a roughly circular orbit would only cause an average stellar radial velocity of around 48 km/h which is slightly above the speed of the fastest human!

However, the effects of this motion can be seen in the emitted spectra of the star as a result of the Doppler effect.

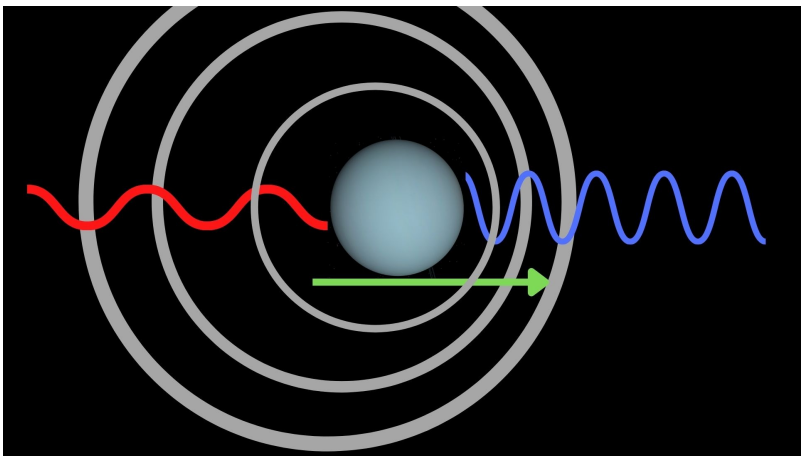

Figure 8.1: The Doppler Effect

Just as you'd hear a car horn at a lower pitch as it moves away from you, the light coming from a receding star would be red-shifted and blue-shifted as it comes towards you. This change in emitted spectra has a periodicity of the orbital period of the star and it can be studied to infer many things about the surrounding exoplanet(s).

Since this is the last method we'll be talking about, you probably need extra motivation, so here are some extra videos to recapture your interest :)

- https://exoplanets.nasa.gov/resources/2285/radial-velocity/
- https://exoplanets.nasa.gov/resources/2337/exoplanet-detection-radial-velocity-method/
- https://www.youtube.com/watch?v=sJ45Gb99KII
- https://www.youtube.com/watch?v=YOS3LrTtpZg
- https://www.youtube.com/watch?v=dQw4w9WgXcQ - Most interesting: personal opinion :)

8.2 Theory

8.2.1 Orbits

As radial velocity involves common references to a few terms, a precursory short discussion on orbital parameters is needed.

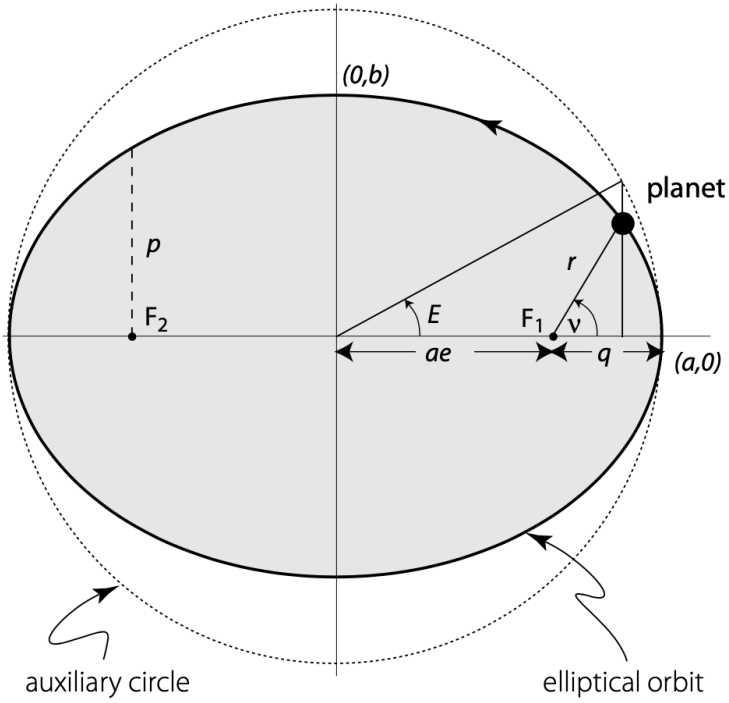

Figure 8.2: A 2-dimensional Elliptical Orbit (Perryman, 2011, p.9)

As in all orbiting systems, both star and planet orbit the common system barycentre. Under

the inverse square law of gravity, each moves in a closed elliptical orbit in inertial space, with the centre of mass at one focus. Such an ellipse is described in polar coordinates (with respect to a focus) by:

$$r = \frac{a(1-e^2)}{1+ecosv} \tag{8.1}$$

or in cartesian coordinates (wrt the centre):

$$\frac{x^2}{a^2} + \frac{y^2}{b^2} = 1 \tag{8.2}$$

The pericentre distance q and apocentre distance Q are given by

$$p = a(1-e) \tag{8.3}$$

$$Q = a(1+e) \tag{8.4}$$

What is v here? As mentioned in an earlier chapter, v(t) (also called f(t)) is the true anomaly, which is the angle between the direction of the pericentre and the current position of the body measured from the barycentric focus of the ellipse. In Figure 7.2, note the direction of the z-axis, and the object's, or rather the star's displacement about the barycentre.

The orbital period can P be related to the relative distance between planet and star, by Kepler's third law, for a relative orbit:

$$P^2 = \frac{4\pi^2}{G(M_p + M_\star)} a_{rel}^3 \tag{8.5}$$

For an absolute orbit, the Star and planet revolve around the common Barycentre. The stellar distance $a_\star$ can be related to P as:

$$P^2 = \frac{4\pi^2(M_p + M_\star)^2}{GM_p^3} a_\star^3 \tag{8.6}$$

and $a : a_p : a_{rel} = M_p : M_\star : (M_\star + M_p)$ with $a_{rel} = a_\star + a_p$

The star's z-coordinate (along the line of sight) can be derived from trigonometry (Observe Fig 7.2) as:

$$z = r(t) \sin i \sin(\omega + v) \tag{8.7}$$

Thus, to find the radial velocity:

$$v_r \equiv \dot{z} = \sin i \left[\dot{r} \sin(\omega + v) + r\dot{v} \cos(\omega + v)\right] \tag{8.8}$$

Some algebraic substitutions for and lead to:

$$v_r = K[\cos(\omega + v) + e\cos\omega] \tag{8.9}$$

where the radial velocity semi-amplitude K of the star is given by:

$$K = \frac{2\pi}{P}\frac{a_\star \sin i}{(1-e^2)^{1/2}} \tag{8.10}$$

hence, v_r as viewed from earth varies between $K[1 - e\cos\omega]$ and $K[1 + e\cos\omega]$.

As there is no way to know a priori the period of the wobble, the radial velocity curve is constructed through repeated sampling over days/weeks. How do we take these samples, and what are the problems associated?

8.2.2 Measurements, Error and Limits

Obtaining the readings

A star's spectrum is made up of many absorption lines, created by the tenuous outer layers of the stellar atmosphere as they absorb some of the continuous light coming from the hot, dense interior.

As you know, Absorption lines are usually seen as dark lines, or lines of reduced intensity, on a continuous spectrum. This is seen in the spectra of stars, where gas (mostly hydrogen) in the outer layers of the star absorbs some of the light from the underlying thermal blackbody spectrum.

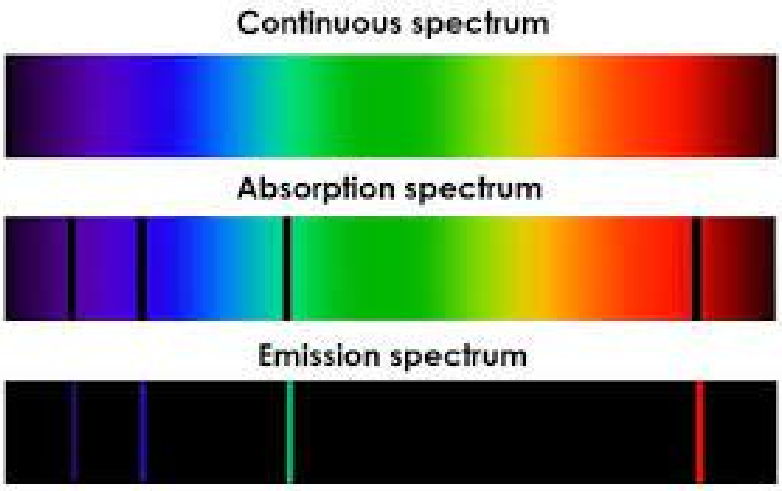

Figure 8.3: Spectrum

You can think of the radial velocity method as measuring the shift of those black lines of the absorption spectrum with time. observing a spectrum like this, with no idea of true intensities whatsoever isn't practical, so we use a spectrograph to split this incoming light into its constituent colours and measure the intensities using corresponding photodetectors.

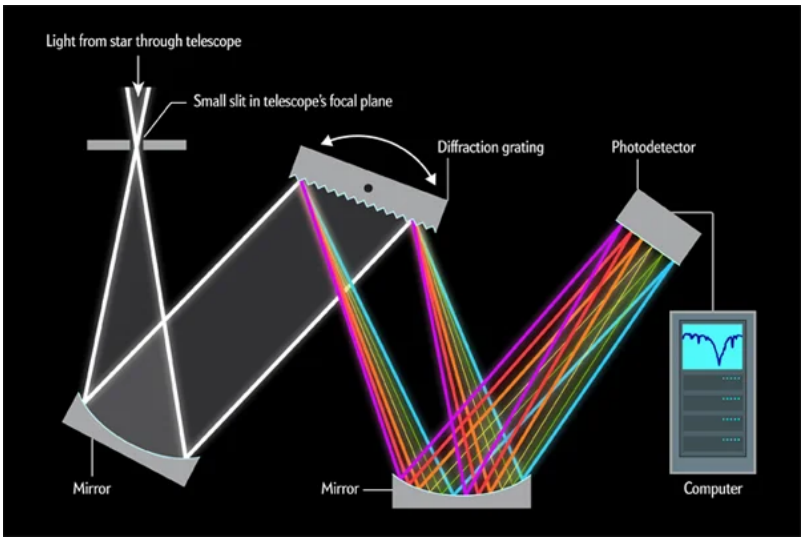

Figure 8.4: Spectrograph

The spectral resolving power of a spectrograph, or the ability to distinguish 2 different wavelengths is an important factor to consider. The diffraction grating in the spectrograph is an Echelle Diffraction Grating used in Littrow Configuration.

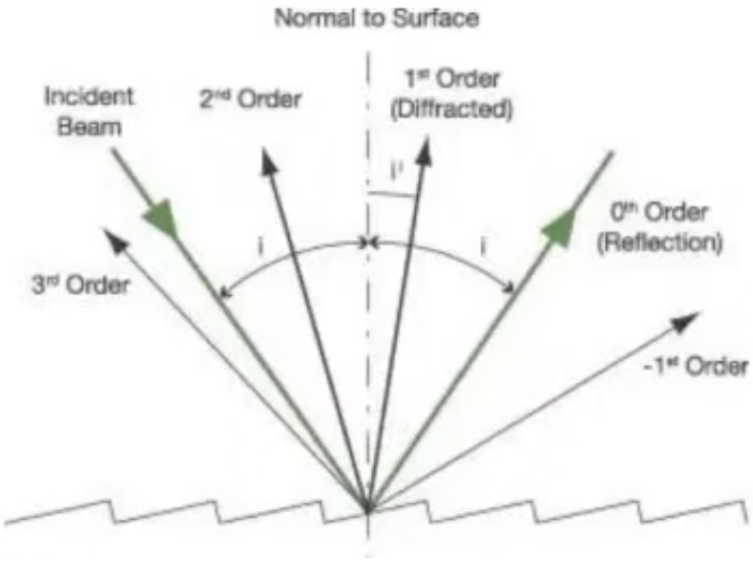

Figure 8.5: Echelle grating

We need the different wavelengths to be as spread-out as possible, for a better resolution, this

is where the angular dispersionn(A) comes in:

$$A = \frac{m}{n\sigma \cos \beta} \tag{8.11}$$

From the above, we can see that the "spread" or angular dispersion is larger for larger orders (m) of diffraction, however, we can see intuitively that the maximum intensity of light will be reflected along the 0th order or central maximas, intensity decreasing with increase in order.
To combat this, the grating is used in Littrow Configuration, which increases the intensity of 1st order difraction patterns and allows us to see them better. This video has an explanation of Littrow configuration. Basically, you orient the echelle grating in such a way that the 0th order reflection is along the incident ray.

From the spectrograph, we get a plot of intensity vs wavelength, as so..

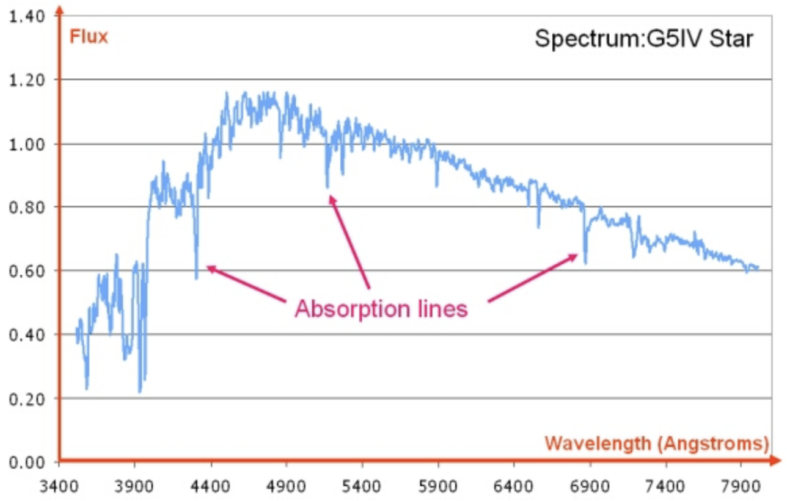

Figure 8.6: Spectrum plot, Credit

This kind of spectrum isn't solely the sun's emission, it has the effects of the earth's motion, the star's gravitational red-shift as the light approaches us, as well as the stellar space motion, all of which must be accounted for and be fitted out.

It is the shift in these dips we measure, but we can't do so without a reference..

Calibration

Gas Cells: The shifts in the absorption lines can be observed by comparing them to the known separations in absorption lines of elemental absorption spectra, such as that of Iodine. Thus, the Iodine absorption spectrum acts as a "scale" for the measurement in question.

The spectrograph used to measure stellar spectra is calibrated using known reference light sources. This calibration ensures that the spectrograph's wavelength scale is accurately aligned.

The stellar light is passed through a glass cell containing iodine which results in a superimposition of both spectra, the combined spectrum is then analyzed to measure the Doppler shifts of the iodine lines relative to their known rest wavelengths, allowing us to measure the shift.

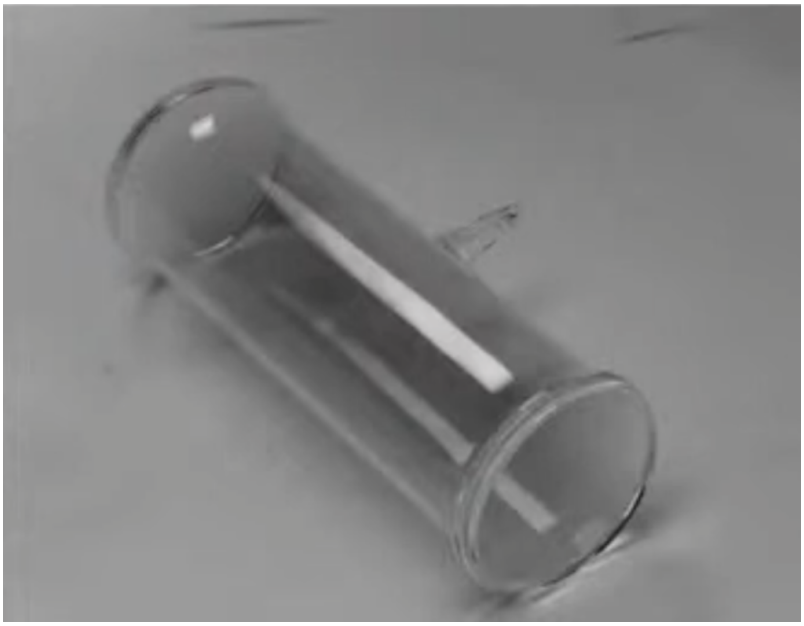

Figure 8.7: Iodine Gas Cell

The Iodine Molecular lines provide a dense forest of absorption lines between 5000 to 6200 Å (Visible range). Most of the central main sequence stars emit heavily in this wavelength band, which is another reason why many missions were aimed at detecting planets around these stars.

The advantages of this method are the high stability and precision of absorption lines, however, there are disadvantages, which include the limited wavelength usage range, variation in spectrum with iodine pressure, and high SNR values needed.

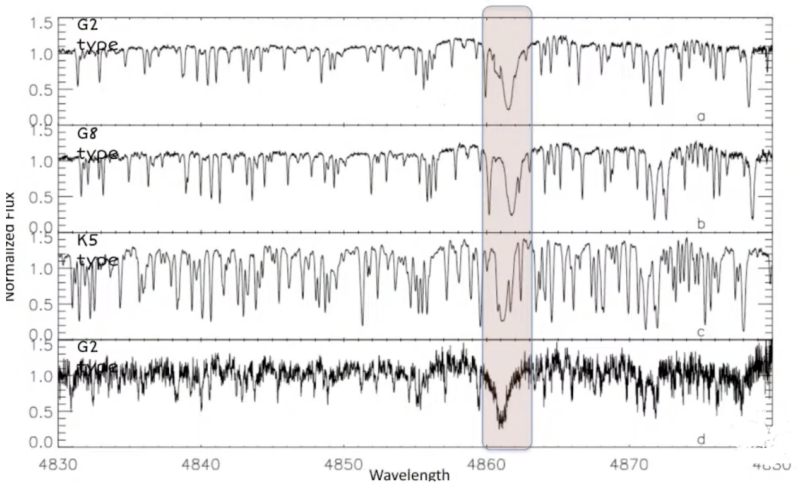

Figure 8.8: Obtained Stellar Spectra

Some interesting things to note:
you'll notice the top and bottom stars are both G2 type stars, the latter's spectrum has more noise which implies a lesser brightness. As the spectral class moves to lower temperatures, the number of absorption lines increase (check G2→G8→K5). [why?]

There are other calibration methods as well, like the **Thorium-Argon method**, which employs a thorium–argon emission lamp as the reference wavelength spectrum.
In its practical implementation, two optical fibres are used to transfer light to the spectrograph, one collecting the stellar light, the other simultaneously recording either a thorium–argon reference spectrum, or the background sky.
The advantages of the thorium–argon lamp for wavelength calibration are the large numbers of strong emission lines over a wide optical to infrared range and the improvement in throughput due to the absence of the iodine absorption cell.

After we measure the shift in wavelength with time, the observed wavelength can be related to the emitted wavelength through the formula for relativistic doppler shift:

$$\lambda_{obs} = \lambda_{em} \frac{(1 + \beta \cos\theta)}{(1 - \beta^2)^{1/2}} \tag{8.12}$$

Where β is v/c, for $v << c$ (which is indeed the case here), If in the observer's reference frame, the source is receding with velocity v at an angle θ relative to the direction from observer to source. due to the large distance, $\theta << \pi/2$, hence this reduces to the classical form:

$$v_r = v \cos\theta \simeq v \simeq \left(\frac{\Delta\lambda}{\lambda_{em}}\right) c \tag{8.13}$$

This gives us a radial velocity curve from the measurements:

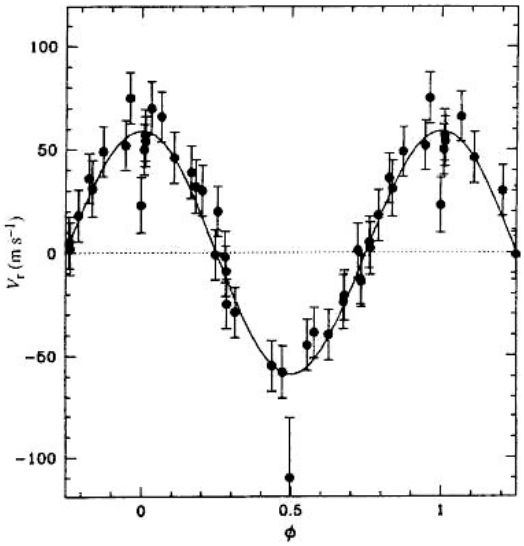

Figure 8.9: Fitted radial velocity curve for 51 Pegasi b. X-axis: Oscillation phase, Y-axis: Radial velocity (m/s). Credit

The accuracies of this method are limited by photon noise, stellar surface noise, wavelength calibration and thermal and the mechanical stability needed.

8.2.3 Radial Velocity Curves and Information Obtained

An ideal radial velocity curve for a star with a single planet would look something like this:

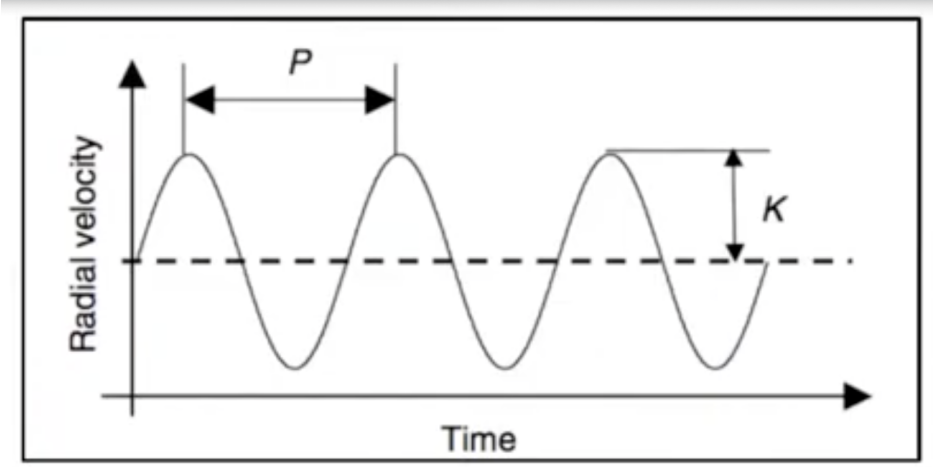

Figure 8.10: Radial Velocity Curve

Radial velocity (Doppler) measurements describe the projected motion, along the line-of-sight, of the primary star as it orbits the system barycentre, hence not all seven Keplerian orbital elements are accessible from the line-of-sight velocity variations alone.

Of the 7 Kepler variables, Ω cannot be determined, also, from the formula of K, only the combination of $a_\star \sin i$ can be found, and not inclination and a separately. K is a function of a, e, P, i, along with a systemic velocity term γ to account for the proper motion, and an instrument-dependant offset, a parameter linearly varying with time, $d(t - t_0)$, we can write the radial velocity of a star due to a single planet as:

$$v_r(t) = K[\cos(\omega + v(t)) + e\cos\omega] + \gamma + d(t - t_0) \tag{8.14}$$

Hence we can model radial velocity curves and vary the parameters for the best fit. Observing the spectrum itself also gives us a lot of clues about possible stellar and planet composition. the minimum mass, $M_p \sin i$ mass can also be found from the observables of K, P, and e.

For a system of n_p planets, the total radial velocity signal can be approximated as a linear sum over n_p terms of the form contained in equation (8.14) giving a total of $5n_p + 1$ Keplerian parameters to be fit, including γ (and optionally d). Advanced algorithms implement planet-planet interactions as well.
But, How do we know it is due to a planet?? A question which probably should have been asked sooner:/

Radial velocity plots may result from changing the radial velocity of a star, but signals could also come up due to stellar activity, Instrumental effects, Earth's atmospheric absorption etc. (mainly stellar activity).

Hence, radial velocity measurements alone aren't enough to conclude the existence of an exoplanet, other analysis methods must be used such as "line bisector analysis", where the "bisector" (a line profile which divides the spectral line into 2 equal parts) of the spectral line as seen in the plot above is analysed for changes in shape and size with radial velocity changes to make sure the exoplanet hypothesis holds. The bottommost point of each spectral line dip would shift with changes in radial velocity, leading to major shifts in the bisector.

8.3 Discoveries

Today around 1050 exoplanets have been discovered through radial velocity. The method is mostly used with transits and other methods to get a more complete picture. It has specialised in detecting planets which, again orbit mostly central main sequence (G and K) stars and cause significant perturbation in the star's spectrum, such as Hot Jupiters and other such large planets. Here are a few examples:

- 51 Pegasi b: This exoplanet, discovered in 1995, was the first confirmed exoplanet orbiting a Sun-like star. It is a hot Jupiter, with a close-in orbit around its host star 51 Pegasi.
- Gliese 581 d: Discovered in 2007, Gliese 581 d was initially considered to be a potentially habitable exoplanet. It orbits the red dwarf star Gliese 581 and is located about 20 light-years away from Earth.

- HD 189733 b: This exoplanet, located approximately 63 light-years away, gained attention due to its blue colour. It was one of the first exoplanets to have its colour directly measured through observations.

Advancement in Technology

9.1 The Future of Exoplanet Detection

As we venture further into the cosmos, the field of exoplanet detection stands on the cusp of revolutionary changes. Advancements in technology and the integration of AI and machine learning promise to accelerate our quest to uncover the secrets of distant worlds. These innovations not only enhance the precision and efficiency of existing methods but also pave the way for entirely new approaches to exploring the universe.

9.1.1 Advancements in Exoplanet Detection Technology

The cutting-edge technologies transforming exoplanet detection are driven by the need to observe fainter objects with greater accuracy and over longer periods. Some of these advancements include the development of ultra-sensitive detectors, more powerful telescopes, and sophisticated data analysis techniques. One key area of progress is in the optimisation of space telescopes equipped with wide-field cameras capable of surveying vast swathes of the sky. These telescopes, such as the James Webb Space Telescope, aim to delve deeper into the cosmos than ever before, capturing the faint signatures of exoplanets orbiting distant stars.

Example:

- **James Webb Space Telescope (JWST)**: Slated to expand our observational capabilities, JWST's suite of instruments will allow astronomers to study exoplanet atmospheres in unparalleled detail, probing the chemical fingerprints of potential habitable conditions.

In addition, ground-based observatories are being upgraded with adaptive optics systems. These systems correct the distortion caused by Earth's atmosphere, dramatically improving image sharpness and allowing for the direct imaging of exoplanets. Moreover, the method of gravitational microlensing is benefiting from vast networks of telescopes coordinated worldwide, enhancing the ability to catch and study the fleeting magnification events that signal the presence of exoplanets.

9.2 Exoplanet Detection Using Machine Learning

Machine Learning: A subset of artificial intelligence (AI) that provides systems with the ability to automatically learn and improve from experience without being explicitly programmed.

The application of AI and machine learning in exoplanet detection is rapidly transforming the field, offering new levels of efficiency and discovery potential. These technologies are adept at processing and analysing the enormous volumes of data produced by telescopes, distinguishing the subtle signs of exoplanets amidst the noise. AI models, once trained on datasets of known exoplanet signals, can autonomously identify similar signals in new data. This capability is particularly valuable in methods like the transit technique, where the detection of small, Earth-like exoplanets requires the analysis of minute changes in starlight.

Beyond data analysis, AI is also facilitating the optimisation of observation schedules for telescopes, ensuring that monitoring efforts are directed efficiently. Machine learning techniques are being used to predict stellar activity, which can help in distinguishing between false positives and genuine exoplanet candidates. This integration of AI and machine learning not only streamlines the detection process but also opens up new possibilities for understanding the nature and diversity of exoplanets, bringing us closer to answering the age-old question of whether we are alone in the universe.

9.2.1 Deep Dive

One fascinating advancement is the use of neural networks for the classification of exoplanet atmospheres. By analysing the spectrum of light that has passed through an exoplanet's atmosphere, AI can identify patterns indicative of chemical compounds, gases, and even weather patterns. This application of machine learning could be crucial in identifying habitable planets and understanding the conditions necessary for life as we know it.

Conclusion and Extra Reading

This long and surely exhausting module has ended right here, but our questions may not. Are we alone? Will we ever know? Where do we go from here? The aim of this module (from my side) wasn't (entirely) to bombard one with information, but more to pique curiosity, and I hope it has done a good job there!

Here are some links you can refer to for extra reading:

- The Exoplanet Handbook, Michael Perryman: http://www.variables.ch/images/Literatur/The_Exoplanet_Handbook_Perryman_Michael.pdf (Amazing read)
- http://spiff.rit.edu/classes/extrasol/lectures/intro_rescue/intro_notes.html (Lectures by Michael Richmond, RIT -> You'll find great lectures of his for all the methods discussed here)